

A Medical Multimodal Large Language Model for Pediatric Pneumonia

Weiwei Tian, Xinyu Huang, Tianhao Cheng, Wen He, Jinwu Fang, Rui Feng, Daoying Geng, Xiaobo Zhang

Abstract—Pediatric pneumonia is the leading cause of death among children under five years worldwide, imposing a substantial burden on affected families. Currently, there are three significant hurdles in diagnosing and treating pediatric pneumonia. Firstly, pediatric pneumonia shares similar symptoms with other respiratory diseases, making rapid and accurate differential diagnosis challenging. Secondly, primary hospitals often lack sufficient medical resources and experienced doctors. Lastly, providing personalized diagnostic reports and treatment recommendations is labor-intensive and time-consuming. To tackle these challenges, we proposed a Medical Multimodal Large Language Model for Pediatric Pneumonia (P2Med-MLLM). This was the first foundation model tailored for patients primarily diagnosed with pediatric pneumonia, capable of handling diverse clinical tasks—such as generating free-text radiology reports and medical records—within a unified framework. Specifically, P2Med-MLLM can process both pure text and image-text data, trained on an extensive and large-scale dataset (P2Med-MD), including real clinical information from 163,999 outpatient and 8,684 inpatient cases. This dataset comprised 2D chest X-ray images, 3D chest Computed Tomography (CT) images, corresponding radiology reports, and outpatient and inpatient records. P2Med-MLLM combined a Large Language Model (LLM) with a vision encoder, fine-tuning them together to handle multiple temporally sequenced and interleaved 2D or 3D images with corresponding radiology reports using a perceiver module. We designed a three-stage training strategy to enable P2Med-MLLM to comprehend medical knowledge

and follow instructions for various clinical tasks. To rigorously evaluate P2Med-MLLM's performance, we developed P2Med-MBench, a benchmark consisting of 642 meticulously verified samples by pediatric pulmonology specialists, covering six clinical decision-support tasks and a balanced variety of diseases. The automated scoring results demonstrated the superiority of P2Med-MLLM. This work plays a crucial role in assisting primary care doctors with prompt disease diagnosis and treatment planning, alleviating patient disease burden, reducing severe symptom mortality rates, and optimizing the allocation of medical resources.

I. INTRODUCTION

In 2021 alone, more than 0.5 million children under the age of five died from Lower Respiratory Infections (LRI) worldwide, accounting for 12% of total deaths [1]. Among LRI, pediatric pneumonia, especially when accompanied by severe symptoms and complications, has the highest morbidity and mortality, particularly in developing countries [2]. Pediatric pneumonia, bronchitis, and asthma share similar symptoms like coughing and wheezing, making prompt diagnosis upon admission very challenging [3]. Limited healthcare resources and a lack of experienced doctors in primary hospitals exacerbate this situation, leading to misdiagnoses and inappropriate treatments.

To meet the growing demands of precision medicine, deep learning-based technologies have emerged for identifying pediatric respiratory diseases [3], [4], early triage [5], and predicting clinical outcomes [6]. Despite achieving or nearing human expert levels, these models primarily treated clinical tasks as simple classification or regression problems, falling short of providing detailed and reliable diagnostic bases and treatment recommendations.

Recently, Multimodal Large Language Models (MLLMs) have experienced exponential growth in general domains [7]–[12], but they were still not fully capable of effectively supporting real-world clinical applications [13]. The essential reason was that, to protect patient privacy, these models were mainly trained on medical textbooks and literature from the internet, without exposure to real and comprehensive medical data. Aligning with human doctors has significantly improved MLLMs' performance across various specialties (*e.g.*, radiology, pathology, ophthalmology, and dermatology) and tasks (*e.g.*, disease diagnosis, medical image generation, medical image caption, medical report generation, medical report summarization, rationale diagnosis, survival prediction, medical image-text retrieval, medical report quality assessment, medical question answering, and medical visual

Manuscript received September 4, 2024. This work was supported in part by the National Natural Science Foundation of China (No.62172101), and in part by the Science and Technology Commission of Shanghai Municipality (No.22511106003, No.23511100602) and Municipal Hospital Frontier Joint Research Project (No.SHDC12024136), which studies on Evaluation Indicator Construction and Clinical Application Management for Diagnostic and Treatment Assistant Large-scale Model for Pediatric Severe Pneumonia. (Xinyu Huang and Tianhao Cheng contributed equally. Corresponding author: Xiaobo Zhang.)

Weiwei Tian, Rui Feng, and Daoying Geng are with the Academy for Engineering and Technology, Fudan University, No. 220 Handan Road, Shanghai 200433, China (e-mail: {wwtian20, fengrui}@fudan.edu.cn, gengdy@163.com).

Xinyu Huang, Tianhao Cheng, and Rui Feng are with the School of Computer Science, Shanghai Key Laboratory of Intelligent Information Processing, Fudan University, No. 2005 Songhu Road, Shanghai 200438, China (e-mail: xinyuhuang20@fudan.edu.cn, thcheng23@m.fudan.edu.cn).

Wen He, Rui Feng, and Xiaobo Zhang are with the Department of Respiratory Medicine, Children's Hospital of Fudan University, No. 399 Wanyuan Road, Shanghai 201102, China (e-mail: hewen@fudan.edu.cn, zhangxiaobo0307@163.com).

Jinwu Fang is with the School of Public Health, Fudan University, No. 130 Dongan Road, Shanghai 200032, China (e-mail: fangjinwu007@126.com).

Daoying Geng is also with the Department of Radiology, Huashan Hospital, Fudan University, No. 12 Wulumuqi Rd. Middle, Shanghai 200040, China.

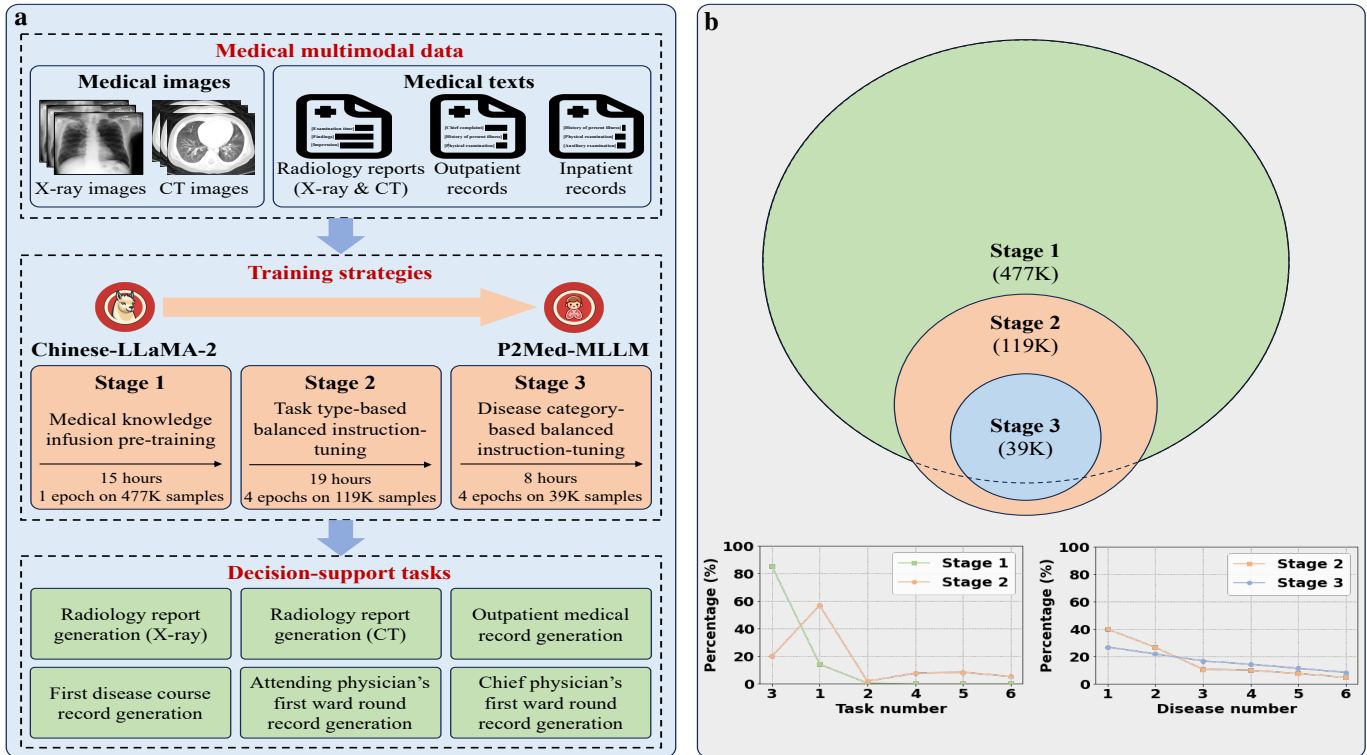


Fig. 1: Overview. (a) The flowchart of this study. (b) The data distribution in different training stages. Note: P2Med-MLLM: Medical Multimodal Large Language Model for Pediatric Pneumonia. CT: Computed Tomography.

question answering) [14]–[29] in the healthcare field. Inspired by the aforementioned work, we aim to explore the feasibility of MLLMs using real clinical data on pediatric pneumonia. Given the complexity of pediatric pneumonia, we mainly face challenges from three aspects:

- **Lack of a large-scale and high-quality multimodal dataset for training:** Due to the rapid physical development of children, their medical imaging, laboratory tests, and demographic data significantly differ from those of adults. Currently, there is a shortage of a large-scale pediatric pneumonia dataset that reflects real clinical scenarios. Moreover, real-world data tend to be noisy and have a long-tailed distribution, which can severely impact model training effectiveness.
- **Lack of a unified and compatible model architecture:** Addressing the diverse clinical needs in the full process of diagnosing and treating pediatric pneumonia requires a model architecture that can efficiently handle different modalities, sequences, and time-series data inputs, and produce outputs for various tasks in a unified manner. Currently, such a compatible model structure is lacking.
- **Lack of a comprehensive and objective evaluation benchmark:** A comprehensive and objective benchmark is crucial for supervising model training and assessing performance. There is a lack of a high-quality evaluation benchmark that covers a wide range of clinical tasks and disease categories.

To address the obstacles of applying MLLMs to pediatric pneumonia, we developed a **Medical Multimodal Large Language Model** tailored for **Pediatric Pneumonia** (P2Med-MLLM, Fig. 1a), which was trained and deployed on a local

server within the hospital environment to ensure data security and privacy.

To effectively train P2Med-MLLM, we constructed the first large-scale **Chinese Medical Multimodal Dataset for Pediatric Pneumonia** (P2Med-MD), covering real clinical information from 163,999 outpatients and 8,684 inpatients. Specifically, we collected comprehensive medical data for patients with a primary diagnosis of pediatric pneumonia, including 2D chest X-ray and 3D chest Computed Tomography (CT) images, corresponding radiology reports, outpatient records, and three-level inpatient records reflecting disease progression [30] (Fig. 1a). During the three training stages, we ensured data quality by deduplication, task type-based balanced sampling, and disease category-based balanced sampling (Fig. 1b).

As for the architecture of P2Med-MLLM, it consisted of three core components: a Large Language Model (LLM, Chinese-LLaMA-2 [31]), a CLIP-pretrained vision encoder [32], and a perceiver module [7]. This design enabled P2Med-MLLM to retain its original capabilities in understanding and generating pure text (outpatient and inpatient records), while also allowing it to interleave multiple 2D chest X-rays or 3D chest CT images with corresponding radiology reports. This facilitated comparative analysis of a patient's radiological examinations over different time points, aligning more closely with clinical practice.

For evaluation, we initialized a **Medical Multimodal Benchmark for Pediatric Pneumonia**, termed P2Med-MBench. This benchmark covered various disease categories and valuable clinical tasks, including radiology report generation (X-ray), radiology report generation (CT), outpatient medical record generation, first disease course record generation, at-

tending physician’s first ward round record generation, and chief physician’s first ward round record generation (Fig. 1a). All real-world data have been meticulously verified by professional pediatric pulmonology specialists to ensure quality and representativeness. Automatic scoring of results generated by P2Med-MLLM and other open-source LLMs on P2Med-MBench, along with a series of ablation studies, demonstrated the superiority of our approach.

Overall, the main contributions of our work are summarized as follows:

- **Construct a large-scale and high-quality multimodal dataset (P2Med-MD):** Based on real clinical scenarios, we developed the first Chinese medical multimodal dataset for patients with a primary diagnosis of pediatric pneumonia. This dataset covered various diseases and clinical tasks.
- **Propose a unified and compatible multimodal model architecture (P2Med-MLLM):** For different clinical tasks, we introduced the first model capable of handling both pure text data (outpatient and inpatient records) and temporally sequenced, interleaved image-text pairs (2D X-rays and 3D CT images, along with corresponding radiology reports).
- **Establish a comprehensive and objective multimodal evaluation benchmark (P2Med-MBench):** To supervise the training process and objectively evaluate different models, we meticulously designed a multimodal benchmark with balanced distributions of diseases and clinical tasks. Extensive quantitative and qualitative experimental results demonstrated the effectiveness of our approach.

II. RESULTS

In this section, we conducted experiments on various tasks, including radiology report generation (X-ray), radiology report generation (Computed Tomography, CT), outpatient medical record generation, first disease course record generation, attending physician’s first ward round record generation, and chief physician’s first ward round record generation. We began by describing the evaluation metrics used for the experiments. Then, we presented the quantitative and qualitative results of our framework on the Medical Multimodal Benchmark for Pediatric Pneumonia (P2Med-MBench).

A. Evaluation Metrics

To evaluate the professional performance of various Medical Multimodal Large Language Model variants for Pediatric Pneumonia (P2Med-MLLM) and baseline models, we utilized 13B Chinese-LLaMA-2 [31] with a one-shot in-context example to automatically score the generated open-ended responses and provide reasons for the given scores. Our pediatric pulmonology specialists meticulously curated a set of examples across tasks and evaluation components based on their clinical expertise. For the most critical evaluation components in a range of tasks, such as impression or diagnosis results, we employed accuracy and comprehensiveness metrics. For other evaluation components, we used accuracy alone. We assessed the quality of the generated answers using a 5-point scale, as

depicted in Fig. 2. The original Chinese version can be found in Fig. S1. The 95% confidence interval for each metric was calculated using the t -distribution.

B. Radiology Report Generation (X-ray)

As shown in Table I, Large Language Models (LLMs) such as Baichuan 2 [33] and Chinese-LLaMA-2 [31] can only process pure texts. In clinical practice, X-ray images were crucial for screening and diagnosing pediatric pneumonia. By incorporating a perceiver with an LLM, P2Med-MLLM can handle sequential 2D X-ray images and generate corresponding radiology reports. Fig. 3 demonstrated that P2Med-MLLM was capable of processing X-ray images taken at different times from the same patient in two conversation turns. The model generated different impressions: “*bronchopneumonia*” (October 29, 2022) and “*bronchopneumonia resolved*” (November 11, 2022), effectively reflecting the patient’s disease progression. The original Chinese results were detailed in Fig. S2.

C. Radiology Report Generation (CT)

In addition to 2D X-ray images, P2Med-MLLM can also generate radiology reports for 3D CT images. As shown in Fig. 3 and Fig. S2, the model successfully identified critical radiological features in the images and recognized underlying diseases.

D. Outpatient Medical Record Generation

Generating outpatient medical records was a challenging and open-ended task that required comprehensive analysis of the outpatient’s chief complaint, history of present illness, and physical examination. As indicated in Table I, the 8B P2Med-MLLM demonstrated significant improvements compared to other LLMs (such as the 7B or 13B Baichuan 2 or Chinese-LLaMA-2). For example, P2Med-MLLM increased the accuracy of preliminary diagnosis from 2.96 to 3.37 and improved the comprehensiveness from 3.26 to 4.17. These results indicated that P2Med-MLLM can generate radiology reports without compromising the language model’s capabilities. Fig. 3 and Fig. S2 showed that P2Med-MLLM can make accurate diagnoses in free-text format and provide highly relevant treatment recommendations and plans, despite missing information “*follow-up appointments as necessary*”.

E. First Disease Course Record Generation

Generating resident physician’s first disease course records for inpatients was more challenging because it required comprehensive analysis of various information, including the history of present illness, physical examination, auxiliary examinations, and clinical history features. As depicted in Table I, compared to the suboptimal models, the 7B or 13B Baichuan 2, P2Med-MLLM showed an improvement in the accuracy and comprehensiveness of admission diagnosis by 0.25 and 0.35, respectively. Qualitatively, as shown in Fig. 3 and Fig. S2, P2Med-MLLM can understand the provided patient information and questions, generating a relatively accurate diagnostic

Instructions: You are a professional radiologist specializing in respiratory radiology. I would like you to compare and evaluate the findings written by radiologists with those automatically generated by AI. Additionally, you need to score the accuracy of the AI-generated findings.

When evaluating the AI-generated findings, you must consider whether the AI system’s findings match the actual clinical conditions and symptoms of the patients as seen in the images.

Using the radiologist-written findings as the ground truth, rated at 5 points, you need to analyze and score the accuracy of the AI-generated findings on a scale of 1 to 5. The specifics of each point are as follows:

- 1 - The information in the AI report is completely incorrect and severely inconsistent with the clinical reality.
- 2 - The AI report contains multiple obvious errors that need to be corrected.
- 3 - About half of the information in the AI report is correct, but it includes several errors that need to be verified.
- 4 - The AI report is mostly accurate, but it may contain a few minor errors or omissions that do not affect the overall understanding.
- 5 - The medical information provided by the AI report is entirely consistent with the physician’s clinical judgment.

Input:
[Radiologist findings]
 The thorax is symmetrical, and the trachea is centered. Both lungs show increased and coarse markings, with patchy exudative shadows seen in the lower lobes of both lungs. The mediastinum is centered with unremarkable contours. The cardiac shadow is not enlarged. Both diaphragms are smooth and depressed, and the costophrenic angles are sharp.
[AI-generated findings]
 The thorax is symmetrical, and the trachea is centered. Both lungs show increased and coarse markings, with a patchy exudative shadow seen in the right lower lung. The hilum shadow is not enlarged, and the hilar angles are clear. The mediastinum is centered with unremarkable contours. The cardiac shadow is not enlarged. Both diaphragms are smooth, and the costophrenic angles are sharp.
Output:
[Accuracy analysis] The AI-generated findings include key descriptions such as “the thorax is symmetrical”, “the trachea is centered”, “both lungs show increased and coarse markings” and “a patchy exudative shadow seen in the right lower lung”. However, it omits the key description of “a patchy exudative shadow seen in the left lower lung”. Overall, the description is relatively accurate.
[Accuracy score] 4

Input:
[Radiologist findings]
 Both lungs show normal translucency, with exudative shadows seen in the middle lobe of the right lung and the lower lobes of both lungs. The trachea and bronchi are unobstructed. No significantly enlarged lymph nodes are seen in the mediastinum. No evident signs of pneumothorax or pleural effusion are seen.
[AI-Generated findings]
 Both lungs show uneven translucency with multiple patchy exudative shadows. The trachea and bronchi are unobstructed. No significantly enlarged lymph nodes are seen in the mediastinum. No evident signs of pneumothorax or pleural effusion are seen.
Output:

Fig. 2: Illustration of the evaluation process (English version). We evaluated model-generated answers using 13B Chinese-LLaMA-2.

TABLE I: Comparison with baseline models in six tasks. Accuracy and Comprehensiveness scores of impression or diagnosis results were reported, representing the key metrics of evaluation. The metrics presented reflected the average scores across all test samples, with 95% confidence intervals in parentheses. The best results were bolded. Task 1 to task 6 represented radiology report generation (X-ray), radiology report generation (CT), outpatient medical record generation, first disease course record generation, attending physician’s first ward round record generation, and chief physician’s first ward round record generation, respectively. The baseline models were two recent Chinese LLMs (Baichuan 2 and Chinese-LLaMA-2).

Method	Size	Year	Task 1		Task 2		Task 3		Task 4		Task 5		Task 6		Average	
			Acc	Comp	Acc	Comp	Acc	Comp	Acc	Comp	Acc	Comp	Acc	Comp		
Baichuan 2 [33]	7B	2023	-	-	-	-	2.29	2.89	3.42	3.64	2.83	3.00	2.67	2.98	2.80	3.13
			(2.07, 2.51)	(2.64, 3.14)	(3.18, 3.66)	(3.40, 3.88)	(2.59, 3.07)	(2.72, 3.28)	(2.48, 2.86)	(2.73, 3.23)	(2.68, 2.92)	(3.00, 3.26)				
Baichuan 2 [33]	13B	2023	-	-	-	-	2.96	3.26	3.48	3.55	3.00	3.43	2.96	3.30	3.10	3.38
			(2.76, 3.16)	(3.01, 3.51)	(3.26, 3.70)	(3.31, 3.79)	(2.76, 3.24)	(3.16, 3.70)	(2.75, 3.17)	(3.03, 3.57)	(2.99, 3.21)	(3.25, 3.51)				
Chinese-LLaMA-2 [31]	7B	2023	-	-	-	-	1.50	1.32	2.07	2.06	2.69	2.56	2.54	2.61	2.20	2.14
			(1.17, 1.83)	(1.03, 1.61)	(1.69, 2.45)	(1.68, 2.44)	(2.44, 2.94)	(2.33, 2.79)	(2.29, 2.79)	(2.36, 2.86)	(2.04, 2.36)	(1.99, 2.29)				
Chinese-LLaMA-2 [31]	13B	2023	-	-	-	-	2.68	2.91	3.26	3.07	2.56	2.41	2.18	2.32	2.67	2.68
			(2.47, 2.89)	(2.69, 3.13)	(2.98, 3.54)	(2.80, 3.34)	(2.28, 2.84)	(2.20, 2.62)	(1.97, 2.39)	(2.11, 2.53)	(2.54, 2.80)	(2.56, 2.80)				
P2Med-MLLM	8B	Ours	3.04	3.09	3.81	3.18	3.37	4.17	3.73	3.99	3.07	3.55	2.88	3.47	3.32	3.57
			(2.75, 3.33)	(2.83, 3.35)	(3.50, 4.12)	(2.97, 3.39)	(3.20, 3.54)	(4.04, 4.30)	(3.47, 3.99)	(3.72, 4.26)	(2.80, 3.34)	(3.24, 3.86)	(2.61, 3.15)	(3.15, 3.79)	(3.21, 3.43)	(3.46, 3.68)

Note: CT: Computed Tomography. LLMs: Large Language Models. Acc: Accuracy. Comp: Comprehensiveness. P2Med-MLLM: Medical Multimodal Large Language Model for Pediatric Pneumonia.

basis, admission diagnosis, and diagnostic and treatment plan in a standardized format. However, some details still needed improvement. For instance, the chest X-ray on October 1, 2023, showed “*bronchitis*”, while the chest X-ray on October 8, 2023, showed “*minor inflammation in both lungs and right upper and lower pulmonary emphysema*”. The most recent examination results should be prioritized. Additionally, there were some errors in the nursing level recommendations and medication guidelines that needed to be addressed.

F. Attending Physician’s First Ward Round Record Generation

Generating attending physician’s first ward round records for inpatients was also a crucial and meaningful task for

generative medical foundation models. This task involved using input clinical history features and additional clinical history and signs to produce the patient’s diagnostic basis, current diagnosis, and diagnostic and treatment plan. In Table I, the 8B P2Med-MLLM outperformed the 13B Baichuan 2 by 0.07 in accuracy and 0.12 in comprehensiveness for the current diagnosis, highlighting the advantages of our model. Fig. 3 and Fig. S2 demonstrated the effectiveness of P2Med-MLLM in generating the three components for this task. However, the generated record still had some shortcomings, such as omitting critical information like abnormal findings in the “*physical examination*” section of the diagnostic basis and the “*neonatal nutritional risk assessment*” in the diagnostic and treatment plan.

Task	Input prompt	P2Med-MLLM prediction	Ground truth
Radiology report generation (X-ray)	Current radiological data is as follows: [Examination time] October 29, 2022 [Examination modality] X-ray [Image] <image> [img] Based on the above information, combined with professional radiological knowledge, generate a report in the format: [Findings] {Your findings based on the images} [Impression] {Your impression based on the images}	[Findings] Both lungs show increased and coarse markings, with a patchy exudative shadow seen in the right lower lung. The mediastinum is centered with unremarkable contours. The cardiac shadow is not enlarged. Both diaphragms are smooth, and the costophrenic angles are sharp. [Impression] Suggestive of bronchopneumonia.	[Findings] Both lungs show increased and coarse markings, with a patchy shadow seen in the right lower lung. The mediastinum is centered with unremarkable contours. The cardiac shadow is not enlarged. Both diaphragms are smooth, and the costophrenic angles are sharp. [Impression] Suggestive of bronchopneumonia.
	Current radiological data is as follows: [Examination time] November 11, 2022 [Examination modality] X-ray [Image] <image> [img] Based on the above information, combined with professional radiological knowledge, generate a report in the format: [Findings] {Your findings based on the images} [Impression] {Your impression based on the images}	[Findings] Both lungs show increased and coarse markings, with a patchy shadow seen in the right lower lung, which has been resolved compared to the scan from October 29, 2022. The mediastinum is centered with unremarkable contours. The cardiac shadow is not enlarged. Both diaphragms are smooth, and the costophrenic angles are sharp. [Impression] Bronchopneumonia resolved.	[Findings] Both lungs show increased and coarse markings, with a patchy shadow seen in the right lower lung, which has been resolved compared to the scan from October 29, 2022. The mediastinum is centered with unremarkable contours. The cardiac shadow is not enlarged. Both diaphragms are smooth, and the costophrenic angles are sharp. [Impression] Bronchopneumonia resolved.
Radiology report generation (CT)	Current radiological data is as follows: [Examination time] March 25, 2021 [Examination modality] CT [Image] <image> [img] Based on the above information, combined with professional radiological knowledge, generate a report in the format: [Findings] {Your findings based on the images} [Impression] {Your impression based on the images}	[Findings] Both lungs show uneven translucency with patchy exudative shadows. The trachea and bronchi are unobstructed. No significantly enlarged lymph nodes are seen in the mediastinum. No evident signs of pneumothorax or pleural effusion are seen. [Impression] Pneumonia.	[Findings] Both lungs show uneven translucency with multiple patchy exudative shadows. The trachea and bronchi are unobstructed. No significantly enlarged lymph nodes are seen in the mediastinum. No evident signs of pneumothorax or pleural effusion are seen. [Impression] Pneumonia.
Outpatient medical record generation	Current outpatient pediatric information is as follows: [Chief complaint] Follow-up for pneumonia. [History of present illness] The pediatric patient continues to have fever, accompanied by cough with hollow sound, slightly diminished energy, and satisfactory night sleep. [Physical examination] The pediatric patient is conscious and responsive, with red lips and normal breathing. The breath sounds of bilateral lung are coarse with phlegm rales. The heart sounds are strong and regular. The abdomen is soft without tenderness. The liver and spleen are not enlarged. The bowel sounds are not hyperactive. The NS is negative. Based on the above information, combined with professional medical knowledge, make a diagnosis in the format: [Preliminary diagnosis] {Your preliminary diagnosis} [Treatment recommendation] {Your treatment recommendation} [Treatment plan] {Your treatment plan}	[Preliminary diagnosis] Pneumonia, acute laryngitis. [Treatment recommendation] 1. Health education: maintain a bland diet, increase water intake, frequent back patting, avoid cross-infection. 2. Seek immediate consultation if severe cough, rapid breathing, cyanosis, persistent high fever, or poor mental response occur. [Treatment plan] 1. Examination: CT – Non-contrast chest CT scan.	[Preliminary diagnosis] Pneumonia, acute laryngitis. [Treatment recommendation] 1. Increase water intake, maintain a bland diet. 2. Seek immediate consultation if severe cough, rapid breathing, or significant lethargy occur. 3. Follow-up appointments as necessary. [Treatment plan] 1. Examination: CT – Non-contrast chest CT scan.
First disease course record generation	Current inpatient pediatric information is as follows: [History of present illness] The pediatric patient (October 1, 2023) presented with paroxysmal cough without obvious inducement 9 days ago ... [Physical examination] The pediatric patient is conscious and responsive, with stable breathing, normal skin elasticity, no rash, no cyanosis of the lips, and no retraction signs. The heart sounds are strong and regular, with no pathological murmurs heard. Bilateral lung movements are symmetrical, with normal tactile fremitus ... [Auxiliary examination] October 1, 2023, Chest X-ray: Bronchitis. October 1, 2023, Blood routine: CRP = 8 mg/L, WBC 10.8*10 ⁹ /L. October 3, 2023, Gastrointestinal ultrasound: Mesenteric lymph nodes are detected. No obvious localized masses are seen in the current observable range of the abdominal cavity ... [Clinical history features] 1. Male, 6 months 13 days old ... Based on the above information, combined with professional medical knowledge, make a diagnosis in the format: [Diagnostic basis] {Your diagnostic basis} [Admission diagnosis] {Your admission diagnosis} [Diagnostic and treatment plan] {Your diagnostic and treatment plan}	[Diagnostic basis] Asthmatic bronchopneumonia: The pediatric patient is a male 6 months 13 days old, admitted for cough and wheezing for 9 days, worsened for 4 days. The physical examination showed the pediatric patient is conscious and responsive, with no cyanosis of the lips, and no retraction signs. The heart sounds are strong and regular, with no pathological murmurs heard. Bilateral lung movements are symmetrical, with normal tactile fremitus. The percussion showed clear sounds. The breath sounds of bilateral lung are coarse with stridor. The abdomen is soft, without gastrointestinal pattern. The liver is palpable below the rib margin. The spleen is not palpable below the rib margin. The bowel sounds are normal. The neurological examination is negative. The chest X-ray showed bronchitis. This diagnosis. [Admission diagnosis] 1. Asthmatic bronchopneumonia. [Diagnostic and treatment plan] 1. Routine respiratory care. 2. Secondary nursing. 3. Complete related examinations: three routine tests, biochemistry, blood culture, sputum culture, sputum pathogens, respiratory pathogens, etc. 4. Closely monitor and follow up on the pediatric patient's condition. 5. Adjust treatment plan according to the pediatric patient's condition changes.	[Diagnostic basis] Asthmatic bronchopneumonia: The pediatric patient is a 6-month-old male infant, admitted for cough and wheezing for 9 days, worsened for 4 days. The physical examination showed bilateral lung movements are symmetrical, with normal tactile fremitus. The percussion showed clear sounds. The breath sounds of bilateral lung are coarse with stridor. The infection indicators were not high in lab tests, and the chest X-ray showed minor inflammation in both lungs, right upper and lower pulmonary lobes. [Admission diagnosis] 1. Asthmatic bronchopneumonia. [Diagnostic and treatment plan] 1. Routine care. 2. Primary nursing. 3. ECG monitoring, nasal cannula oxygen therapy. 2. Cefepime/Sulbactam for anti-infection, Methylprednisolone Sodium Succinate for anti-inflammation, and symptomatic nebulization therapy with Ridesonide, Ipratropium Bromide, and Terbutaline. 3. Complete relevant auxiliary examinations, and adjust the treatment plan according to the pediatric patient's condition.
Attending physician's first ward round record generation	Current inpatient pediatric information is as follows: [Clinical history features] 1. Admitted for "cough and nasal discharge for 3 days". 2. History of present illness: The pediatric patient is an infant of 38+5 weeks gestation ... 3. Physical examination: The pediatric patient appears as a full-term infant, responsive ... 4. Auxiliary examination: October 13, 2023, Blood routine emergency: C-reactive protein < 8 mg/L, Hemoglobin 130 g/L ... [Additional clinical history and signs] The pediatric patient's blood oxygen is stable under nasal cannula oxygen, still coughing with sputum, without rapid breathing, fever, or convulsions. The milk intake is achieved, with no nausea or vomiting. The urination and defecation are normal. Physical examination: The throat is mildly congested. Based on the above information, combined with professional medical knowledge, make a diagnosis in the format: [Diagnostic basis] {Your diagnostic basis} [Current diagnosis] {Your current diagnosis} [Diagnostic and treatment plan] {Your diagnostic and treatment plan}	[Diagnostic basis] Neonatal pneumonia: The pediatric patient is an infant of 38+5 weeks gestation, with birth weight of 3150 grams and wheezing for 3 days, worsened for contacting with an elder sister diagnosed with "mycoplasma pneumoniae". The patient developed nasal discharge and significantly worsened cough with sputum, but no fever. Combined with outpatient chest X-ray results, thus diagnosed. [Current diagnosis] Neonatal pneumonia. [Diagnostic and treatment plan] 1. Provide ECG and blood oxygen monitoring. 2. Provide appropriate feeding with neonatal formula, and nebulization therapy. 2. Adjust treatment plan according to the pediatric patient's condition changes.	[Diagnostic basis] Neonatal pneumonia: The pediatric patient was admitted for cough and nasal discharge for 3 days. Physical examination showed the breath sounds of bilateral lungs are coarse with phlegm rales, combined with chest X-ray results, thus diagnosed. [Current diagnosis] Neonatal pneumonia. [Diagnostic and treatment plan] 1. Provide ECG and blood oxygen monitoring and close monitoring of vital signs. 2. Considering the possibility of respiratory viral infection given the non-elevated blood count, temporary symptomatic therapies such as nebulization for suctioning and expectoration are provided. Monitoring and following up on test results is essential to timely adjust treatment plan and reassess the pediatric patient's condition. 3. Provide appropriate feeding with neonatal formula and monitor feeding to avoid choking. 4. The pain score is 2, indicated low risk in neonatal nutritional risk assessment.
Chief physician's first ward round record generation	Current inpatient pediatric information is as follows: [Clinical history features] 1. The pediatric patient is a female of 1 month and 25 days old ... 2. History of present illness: The pediatric patient presented with pharyngeal gurgling without obvious inducement 5 days ago ... 3. Physical examination: The pediatric patient is conscious and responsive ... 4. Auxiliary examination: December 22, 2021, Blood gas (Neonatal): C-LAC 2.7 mmol/L ... [Additional clinical history and signs] The pediatric patient is placed in a small bed with nasal cannula oxygen (2L 25%), maintaining percutaneous oxygen saturation above 95%, accompanied by pharyngeal gurgling, wheezing, and obvious cough, with occasional paroxysmal cough. The pediatric patient presents with occasional rapid breathing, no grunting or foam. The planned milk intake is achieved without vomiting or abdominal distension. The pediatric patient has 4 stools and a urine output of 4.14 mL/kg in 24 hours. Based on the above information, combined with professional medical knowledge, make a diagnosis in the format: [Diagnostic basis] {Your diagnostic basis} [Current diagnosis] {Your current diagnosis} [Diagnostic and treatment plan] {Your diagnostic and treatment plan}	[Diagnostic basis] Bronchopneumonia: The pediatric patient is a female of 1 month and 25 days old, admitted for "pharyngeal gurgling with cough and wheezing for 5 days, worsened for 1 day". Physical examination showed the breath sounds of bilateral lungs are coarse with wheezing and a few coarse rales. Combined with chest X-ray results, thus diagnosed. 2. Hemangioma: Physical examination showed a 1.5x1.5cm red hemangioma on the scalp, thus diagnosed. [Current diagnosis] 1. Bronchopneumonia. 2. Hemangioma. [Diagnostic and treatment plan] 1. Routine respiratory care. 2. Secondary nursing. 3. Complete related examinations: three routine tests, liver and kidney function tests, myocardial enzyme spectrum, blood gas analysis, blood culture, sputum pathogens, etc. 3. Rocophin for anti-infection, nebulization therapy, and Mucosolvan for phlegm and asthma. 4. Timely adjust treatment plan according to the pediatric patient's condition changes.	[Diagnostic basis] 1. Bronchopneumonia: The pediatric patient presented with cough and wheezing, requiring nasal cannula respiratory support. Physical examination showed obvious wheezing and a few coarse rales. Combined with chest X-ray results, thus diagnosed. 2. Hemangioma: A hemangioma was seen on the scalp of the pediatric patient, thus diagnosed. [Current diagnosis] 1. Bronchopneumonia. 2. Hemangioma. [Diagnostic and treatment plan] 1. Following a reduction in high-flow nasal cannula oxygen yesterday, the pediatric patient maintains adequate percutaneous oxygen saturation. Respiratory support is adjusted to nasal cannula oxygen. Increased cough and sputum are noted. Ensure proper respiratory management, and timely relieve blood gas analysis and complete relevant examinations as necessary. 2. Closely monitor and follow up on the pediatric patient's test results to timely adjust treatment plan.

Fig. 3: Qualitative examples of six different evaluation tasks (English version). We presented input prompts along with answers generated by P2Med-MLLM and the target ground truth. The green color in the figure highlighted correct predictions, the red color indicated errors, and the blue color denoted neglected parts. Note: P2Med-MLLM: Medical Multimodal Large Language Model for Pediatric Pneumonia. CT: Computed Tomography.

G. Chief Physician's First Ward Round Record Generation

The task of generating chief physician's first ward round records for inpatients was similar to that of generating attending physician's first ward round records. As shown in Table I, although the 8B P2Med-MLLM maintained advantages in

most tasks, components, and metrics, it fell behind the 13B Baichuan 2 by 0.08 in accuracy for the current diagnosis in this specific task. This was remarkable especially considering that, for the baseline LLMs, namely Baichuan 2 and Chinese-LLaMA-2, the 13B models significantly outperformed the 7B models. It not only demonstrated that more model parameters can lead to further performance improvements, but also

indicated the potential of LLMs that can be further simulated by scaling up the models. Due to computational resource constraints, we opted for the largest model size of 8B to balance performance. Fig. 3 and Fig. S2 showed that our model provided correct answers in most components, except for the incorrect addition of “congenital” in the diagnosis of hemangioma and the omission of the “nasal cannula oxygen” keyword in the components of the diagnostic basis and diagnostic and treatment plan.

III. DISCUSSION

A. Impact of Different Stages and Modalities in P2Med-MLLM

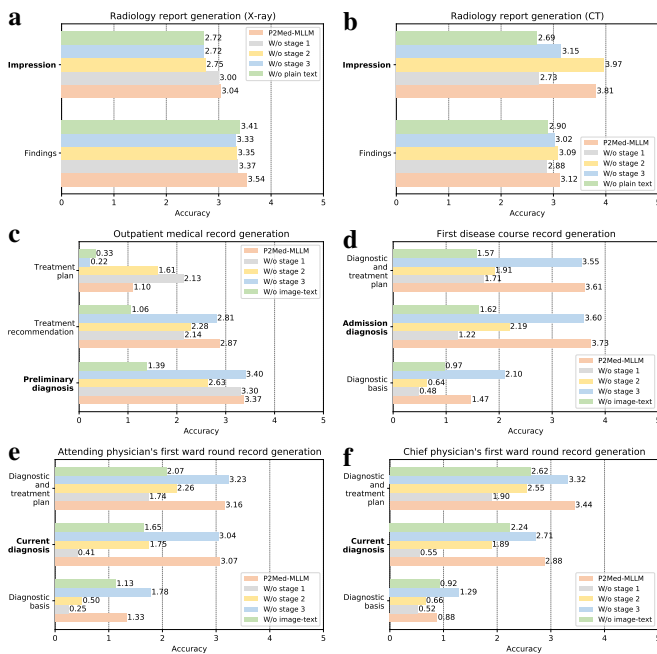


Fig. 4: An ablation study of P2Med-MLLM by removing single stage or modality. We compared six different tasks (a-f) using the accuracy score, with the most crucial evaluation components highlighted in bold. Stage 1 to stage 3 represented medical knowledge infusion pre-training, task type-based balanced instruction-tuning, and disease category-based balanced instruction-tuning, respectively. Note: P2Med-MLLM: Medical Multimodal Large Language Model for Pediatric Pneumonia. CT: Computed Tomography.

To investigate the impact of different stages and modalities, we provided a thorough ablation study of the Medical Multimodal Large Language Model for Pediatric Pneumonia (P2Med-MLLM) by removing single stage or modality. The results were shown in Table II and Fig. 4.

First, we investigated the impact of different training stages on the most critical evaluation components of each task, specifically impression or diagnosis results (columns Full and A-C in Table II). We found that each stage contributed to performance improvement, demonstrating the significance of medical knowledge infusion pre-training, task type-based balanced instruction tuning, and disease category-based balanced

instruction tuning in multi-task clinical decision supports. Specifically, the importance of the three stages, in descending order, were: stage 1, stage 2, and stage 3, respectively.

In addition to the three-stage training strategy, we also evaluated the impact of different modalities, that is, plain text and image-text data. By comparing column Full with columns D and E in Table II, respectively, we observed that removing either modality adversely affected the performance of the other (at least 0.6 on average). These results suggested that tasks involving both modalities were mutually beneficial to some extent. Notably, image-text tasks had a more significant influence on plain text tasks.

Next, as shown in Fig. 4, we explored the performance of P2Med-MLLM across different stages and modalities for all evaluation components of each task. Compared to incomplete stages and modalities, P2Med-MLLM demonstrated significant advantages. Specifically, P2Med-MLLM outperformed others in 4 out of the 6 most crucial evaluation components and in 9 out of 16 evaluation components overall. These observations suggested that while P2Med-MLLM achieved the best results, some evaluation components, such as diagnostic basis and treatment plan, still showed room for improvement. We believed the reason behind this was that the ground truth for these open-ended evaluation components was inherently diverse, making automatic scoring with language models more challenging. Therefore, we focused primarily on the most crucial and standardized evaluation components of each task.

B. Impact of Different Tasks in P2Med-MLLM

Traditional methods typically involved training a network on a subset for a specific medical task. While intuitive, such a training strategy significantly increased computational complexity. To demonstrate the effectiveness of P2Med-MLLM trained jointly on multiple tasks, we compared it with multiple single-task dedicated networks on the most crucial evaluation components using accuracy and comprehensiveness metrics. As shown in Fig. 5, joint training by P2Med-MLLM yielded substantial performance improvements, particularly in tasks such as radiology report generation (Computed Tomography, CT), outpatient medical record generation, and chief physician’s first ward round record generation. We utilized a generative network to unify all tasks, and this flexible structure ensured performance while easily extending to new tasks. It was valuable in the real world for assisting clinicians in completing multiple tasks.

C. Impact of Different Conversation Forms in P2Med-MLLM

We found that during a single outpatient or inpatient visit for each patient, there may be multiple scans for the same imaging modality, reflecting changes in the patient’s condition. Thus, for the radiology report generation task, we constructed a multi-round conversation using all scans of the same imaging modality from a single visit, arranged in chronological order. Using X-ray scans as an example, we compared the performance of models with and without multi-round conversations. As shown in Table III, “w/o MRC” indicated treating each

TABLE II: An ablation study of P2Med-MLLM by removing single stage or modality. Accuracy and Comprehensiveness scores of impression or diagnosis results were reported, representing the key metrics of evaluation. The metrics presented reflected the average scores across all test samples, with 95% confidence intervals in parentheses. The best results were bolded. Stage 1 to stage 3 represented medical knowledge infusion pre-training, task type-based balanced instruction-tuning, and disease category-based balanced instruction-tuning, respectively.

Task description	Metric	Full P2Med-MLLM	A W/o stage 1	B W/o stage 2	C W/o stage 3	D W/o plain text	E W/o image-text
Radiology report generation (X-ray)	Accuracy	3.04 (2.75, 3.33)	3.00 (2.74, 3.26)	2.75 (2.48, 3.02)	2.72 (2.45, 2.99)	2.72 (2.45, 2.99)	-
	Comprehensiveness	3.09 (2.83, 3.35)	3.12 (2.87, 3.37)	2.71 (2.45, 2.97)	2.69 (2.42, 2.96)	2.62 (2.35, 2.89)	-
Radiology report generation (CT)	Accuracy	3.81 (3.50, 4.12)	2.73 (2.45, 3.01)	3.97 (3.70, 4.24)	3.15 (2.92, 3.38)	2.69 (2.38, 3.00)	-
	Comprehensiveness	3.18 (2.97, 3.39)	2.79 (2.50, 3.08)	3.46 (3.24, 3.68)	3.40 (3.19, 3.61)	2.79 (2.48, 3.10)	-
Outpatient medical record generation	Accuracy	3.37 (3.20, 3.54)	3.30 (3.04, 3.56)	2.63 (2.26, 3.00)	3.40 (3.21, 3.59)	-	1.39 (1.00, 1.78)
	Comprehensiveness	4.17 (4.04, 4.30)	3.39 (3.13, 3.65)	2.77 (2.40, 3.14)	4.16 (4.03, 4.29)	-	1.47 (1.07, 1.87)
First disease course record generation	Accuracy	3.73 (3.47, 3.99)	1.22 (0.85, 1.59)	2.19 (1.80, 2.58)	3.60 (3.30, 3.90)	-	1.62 (1.21, 2.03)
	Comprehensiveness	3.99 (3.72, 4.26)	1.14 (0.79, 1.49)	2.12 (1.76, 2.48)	3.44 (3.14, 3.74)	-	1.75 (1.31, 2.19)
Attending physician’s first ward round record generation	Accuracy	3.07 (2.80, 3.34)	0.41 (0.18, 0.64)	1.75 (1.40, 2.10)	3.04 (2.76, 3.32)	-	1.65 (1.28, 2.02)
	Comprehensiveness	3.55 (3.24, 3.86)	0.44 (0.20, 0.68)	2.13 (1.71, 2.55)	3.21 (2.90, 3.52)	-	1.93 (1.51, 2.35)
Chief physician’s first ward round record generation	Accuracy	2.88 (2.61, 3.15)	0.55 (0.31, 0.79)	1.89 (1.57, 2.21)	2.71 (2.42, 3.00)	-	2.24 (1.87, 2.61)
	Comprehensiveness	3.47 (3.15, 3.79)	0.64 (0.36, 0.92)	2.43 (2.03, 2.83)	2.98 (2.66, 3.30)	-	2.62 (2.20, 3.04)
Average	Accuracy	3.32 (3.21, 3.43)	1.87 (1.72, 2.02)	2.53 (2.38, 2.68)	3.10 (2.99, 3.21)	2.71 (2.51, 2.91)	1.72 (1.53, 1.91)
	Comprehensiveness	3.57 (3.46, 3.68)	1.92 (1.77, 2.07)	2.60 (2.46, 2.74)	3.31 (3.20, 3.42)	2.71 (2.51, 2.91)	1.94 (1.73, 2.15)

Note: P2Med-MLLM: Medical Multimodal Large Language Model for Pediatric Pneumonia. CT: Computed Tomography.

scan as an independent single-round conversation. Although P2Med-MLLM and “w/o MRC” achieved comparable results in the evaluation component of findings, adopting multi-round conversations showed a notable advantage in the most crucial evaluation component of impression, exceeding in both accuracy and comprehensiveness metrics by at least 0.37. This demonstrated that the temporal information was critical to perform radiological diagnosis.

D. Impact of Different Large Language Models in P2Med-MLLM

In this subsection, we explored different Large Language Models (LLMs) in P2Med-MLLM using the Medical Multimodal Benchmark for Pediatric Pneumonia (P2Med-MBench). Specifically, we compared models based on Baichuan 2 [33]

and Chinese-LLAMA-2 [31]. The results in Table IV showed that the Chinese-LLAMA-2-based model significantly outperformed Baichuan 2-based model on average and most tasks, except for the outpatient medical record generation task. Therefore, we chose Chinese-LLAMA-2 as the Large Language Model (LLM) for P2Med-MLLM.

IV. OUTLOOK

Multimodal Large Language Models (MLLMs) have brought substantial advancements in the healthcare field. In this study, we preliminarily explored and demonstrated the feasibility of securely and effectively training and deploying a MLLM on private hospital data, specifically focusing on real clinical scenarios involving patients with a primary diagnosis of pediatric pneumonia. Our work encompassed the entire process, from data collection and cleaning to model construction

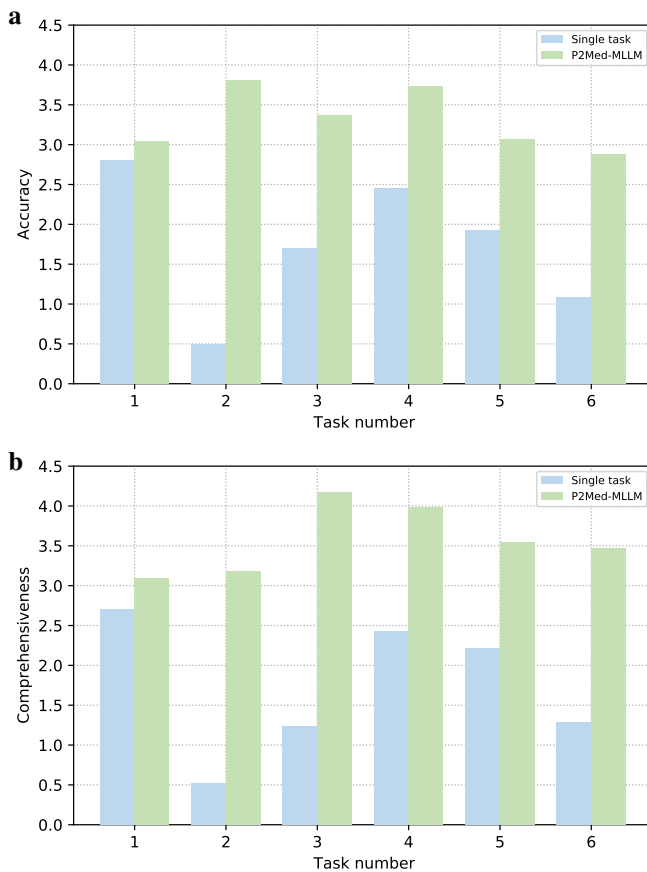


Fig. 5: Performance comparison between multiple single-task dedicated networks and a unified network trained jointly on multiple tasks (P2Med-MLLM). Accuracy (a) and Comprehensiveness (b) scores of impression or diagnosis results were reported, representing the key metrics of evaluation. Task 1 to task 6 represented radiology report generation (X-ray), radiology report generation (CT), outpatient medical record generation, first disease course record generation, attending physician’s first ward round record generation, and chief physician’s first ward round record generation, respectively. Note: P2Med-MLLM: Medical Multimodal Large Language Model for Pediatric Pneumonia. CT: Computed Tomography.

and evaluation, offering a valuable reference for researchers in the interdisciplinary of artificial intelligence for medicine. We built the largest Chinese Medical Multimodal Dataset for Pediatric Pneumonia (P2Med-MD) so far. Different from previous efforts, the Medical Multimodal Large Language Model for Pediatric Pneumonia (P2Med-MLLM) employed a unified framework that supported both pure text data (outpatient and inpatient records) and temporally sequenced, interleaved 2D or 3D medical images alongside radiology reports, aligning more closely with clinical practice. P2Med-MLLM could potentially serve as a clinical assistant, helping doctors enhance diagnostic and treatment efficiency, providing personalized recommendations for pediatric pneumonia patients, and optimizing clinical workflows.

Despite the progress achieved in our research, there are several limitations. Firstly, for complicated and open-ended clin-

TABLE III: An ablation study of P2Med-MLLM in radiology report generation (X-ray) task. The metrics presented reflected the average scores across all test samples in radiology report generation (X-ray) task, with 95% confidence intervals in parentheses. The best results were bolded.

Method	Findings	Impression	
	Accuracy	Accuracy	Comprehensiveness
P2Med-MLLM	3.54 (3.41, 3.67)	3.04 (2.75, 3.33)	3.09 (2.83, 3.35)
W/o MRC	3.49 (3.37, 3.61)	2.67 (2.42, 2.92)	2.53 (2.35, 2.71)

Note: P2Med-MLLM: Medical Multimodal Large Language Model for Pediatric Pneumonia. MRC: Multi-Round Conversations.

ical tasks, such as generating diagnostic bases and treatment plans in medical records, the performance of P2Med-MLLM still falls short of real clinical applications. Additionally, the automatic scoring system lacks robustness, highlighting the need for more objective evaluation metrics. Secondly, this study only includes patients primarily diagnosed with pediatric pneumonia. Future work could extend the objects to cover all respiratory diseases, or even the entire spectrum of general medicine across all age groups. Thirdly, the study is limited to a single-center cohort, and data collection from multiple healthcare institutions and countries would enhance diversity and generalizability. Lastly, as this is a retrospective study, future research could explore prospective studies.

V. METHODS

In this section, we provided a detailed description of our self-built dataset, the medical multimodal Large Language Model (LLM), and the implementation details.

A. Medical Multimodal Dataset for Pediatric Pneumonia (P2Med-MD)

Currently, the medical domain faces a significant shortfall in multimodal datasets that accurately reflect real-world clinical scenarios, a crucial element for training a practical medical multimodal LLM. To bridge this gap, we constructed a high-quality, large-scale Chinese **Medical Multimodal Dataset for Pediatric Pneumonia (P2Med-MD)**, through human-machine interaction. P2Med-MD focused on pediatric patients with a primary diagnosis of pneumonia. Here, we started by providing an overview of P2Med-MD in Sec V-A.1. It consisted of three sets, medical knowledge infusion, task type-based balanced sampling, and disease category-based balanced sampling, corresponding to Sec V-A.2, V-A.3, and V-A.4, respectively. These parts were utilized for different training stages described in Sec V-B. In Sec V-A.5, we introduced a new **Medical Multimodal Benchmark for Pediatric Pneumonia**, termed P2Med-MBench, which encompasses six tasks, e.g., radiology report generation (X-ray), radiology report generation (Computed Tomography, CT), outpatient medical record generation, first disease course record generation, attending physician’s first ward round record generation, and chief physician’s first ward round record generation. These tasks

TABLE IV: An ablation study of P2Med-MLLM with different LLMs. Accuracy and Comprehensiveness scores of impression or diagnosis results were reported, representing the key metrics of evaluation. The metrics presented reflected the average scores across all test samples, with 95% confidence intervals in parentheses. The best results were bolded. Task 1 to task 6 represented radiology report generation (X-ray), radiology report generation (CT), outpatient medical record generation, first disease course record generation, attending physician’s first ward round record generation, and chief physician’s first ward round record generation, respectively.

Method	Task 1		Task 2		Task 3		Task 4		Task 5		Task 6		Average	
	Acc	Comp	Acc	Comp	Acc	Comp	Acc	Comp	Acc	Comp	Acc	Comp	Acc	Comp
Baichuan 2 [33]	2.87 (2.62, 3.12)	2.78 (2.53, 3.03)	2.89 (2.58, 3.20)	2.56 (2.41, 2.71)	3.41 (3.19, 3.63)	4.19 (3.99, 4.39)	2.55 (2.12, 2.98)	2.62 (2.18, 3.06)	2.78 (2.42, 3.14)	3.15 (2.75, 3.55)	2.38 (2.02, 2.74)	2.77 (2.37, 3.17)	2.81 (2.67, 2.95)	3.01 (2.87, 3.15)
Chinese-LLaMA-2 [31]	3.04 (2.75, 3.33)	3.09 (2.83, 3.35)	3.81 (3.50, 4.12)	3.18 (2.97, 3.39)	3.37 (3.20, 3.54)	4.17 (4.04, 4.30)	3.73 (3.47, 3.99)	3.99 (3.72, 4.26)	3.07 (2.80, 3.34)	3.55 (3.24, 3.86)	2.88 (2.61, 3.15)	3.47 (3.15, 3.79)	3.32 (3.21, 3.43)	3.57 (3.46, 3.68)

Note: P2Med-MLLM: Medical Multimodal Large Language Model for Pediatric Pneumonia. LLMs: Large Language Models. CT: Computed Tomography. Acc: Accuracy. Comp: Comprehensiveness.

were designed to monitor the development of the medical multimodal LLM.

1) *Overview*: The study was approved by the Ethics Committee of Children’s Hospital, Fudan University (2022-307A, approved November 22, 2022). For participants admitted before November 22, 2022, informed consent was waived; for those admitted on or after November 22, 2022, informed consent was obtained. In this retrospective study, we collected the outpatient information of 163,999 patients and the inpatient information of 8,684 patients who were admitted to Children’s Hospital of Fudan University between August 26, 2016 to November 1, 2023. Outpatient information included outpatient medical records, and chest X-ray and CT scans along with corresponding radiology reports. Inpatient information comprised three-level round records formed by first disease course records, attending physician’s first ward round records, and chief physician’s first ward round records, as well as chest X-ray and CT scans with corresponding radiology reports. The built dataset altogether contained 67,616 chest X-ray examinations and 2,321 chest CT examinations along with their respective radiology reports, 684,758 outpatient medical records, 9,180 first disease course records, 9,993 attending physician’s first ward round records, and 6,426 chief physician’s first ward round records. More details were given in Table V. Fig. 6 illustrated the distribution of gender, age, and image modalities in P2Med-MD.

2) *Stage 1: Medical Knowledge Infusion Data*: Considering the complexity of inpatient records, stage 1 injected medical knowledge into the general model by learning from all radiology image-report pairs (including X-ray and CT) and simple outpatient medical records. Fig. 7a depicted the disease categories derived from the impression in X-ray radiology reports, with each category comprising over 100 samples during stage 1. Fig. 7c displayed the disease categories extracted from the impression in CT radiology reports, each with more than 10 samples. And Fig. 7d outlined the disease categories identified from the preliminary diagnosis in outpatient medical records, each encompassing over 400 samples.

However, we observed a significant amount of repetitive descriptions within the outpatient records. Prior researches [34]–[37] have demonstrated that repetition in training data can degrade model performance. Thus, it was crucial to perform deduplication to ensure the quality of outpatient records. The data deduplication scheme employed in previous studies [38]–

[40] typically relied on non-whitespace exact text matching, which was suboptimal due to the diverse writing styles of different doctors. [41] indicated that near-deduplication could enhance performance. We followed this pipeline that largely inherited the settings from CodeParrot [42]. It involved calculating MinHashes [43] of all outpatient records and applying Locally Sensitive Hashing (LSH) to cluster records based on their MinHash fingerprints. During the LSH phase, similar outpatient records were grouped into the same buckets, thereby identifying them as duplicates. From each group of duplicates, only one record was retained. Fig. 7e illustrated the disease distribution post-deduplication of these outpatient medical records.

3) *Stage 2: Task Type-Based Balanced Sampling Data*: To ensure the model effectively followed diverse task instructions, we curated a variety of instruction-following data covering six distinct tasks in stage 2. Given the two orders of magnitude difference in sample volumes between outpatient and inpatient medical records, it was essential to balance the number of outpatient and inpatient records, as the generative model was sensitive to data imbalances. By looping through disease categories with sample sizes between 325 and 5,000 in outpatient records of stage 1, a maximum of 500 samples per category were sampled without repetition until the total sample size was balanced with that of inpatient records. Due to the multi-label nature of the preliminary diagnosis in outpatient records, the sampled data included a broader range of disease categories. Fig. 7a, 7c, 7f, 7h, 7i, and 7j depicted the distribution of disease categories for six tasks during stage 2. Specifically, Fig. 7h, 7i, and 7j illustrated the disease categories extracted from the admission diagnosis or current diagnosis in three-level inpatient medical records, each category featuring over 40 samples.

4) *Stage 3: Disease Category-Based Balanced Sampling Data*: We observed considerable differences in the distribution of disease categories per task in stage 2, potentially impairing the performance of the generative model. To mitigate the long-tail problem, it was essential to perform balanced sampling of disease categories in stage 3. For X-ray image-report pairs, we sampled up to 500 samples per category from those with sample sizes ranging from 100 to 2,000. All CT image-report pairs were included due to the relatively smaller sample size. For outpatient medical records, we sampled up to 200 samples per category from those identified in stage 1 with sample

TABLE V: Description of the P2Med-MD. Stage 1 to stage 3 represented medical knowledge infusion pre-training, task type-based balanced instruction-tuning, and disease category-based balanced instruction-tuning, respectively.

Task number	Task description	Total	Stage 1	Stage 2	Stage 3	Test set
1	Radiology report generation (X-ray)	67,616	67,495	67,495	14,461	121
2	Radiology report generation (CT)	2,321	2,200	2,200	2,200	121
3	Outpatient medical record generation	684,758	407,185	23,560	10,200	100
4	First disease course record generation	9,180	-	9,080	3,255	100
5	Attending physician’s first ward round record generation	9,993	-	9,893	4,713	100
6	Chief physician’s first ward round record generation	6,426	-	6,326	3,828	100

Note: P2Med-MD: Medical Multimodal Dataset for Pediatric Pneumonia. CT: Computed Tomography.

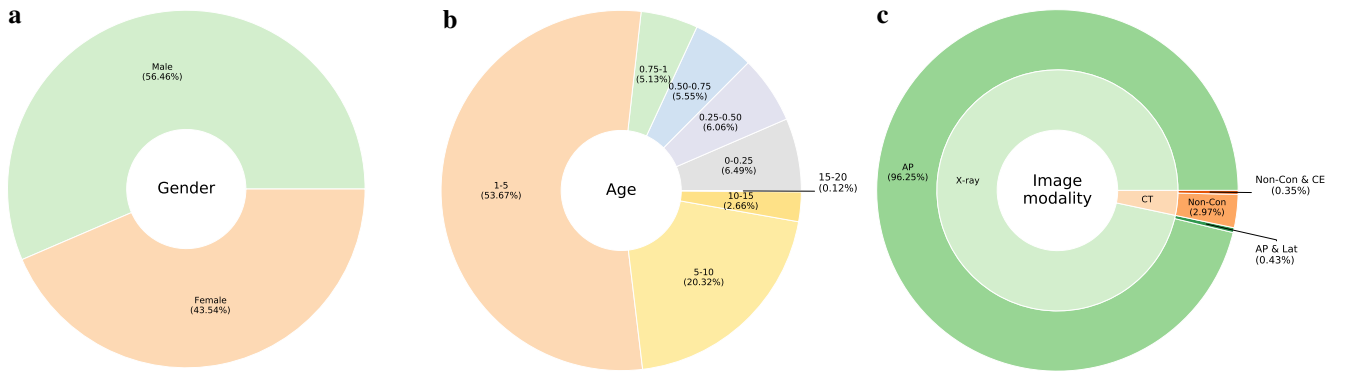


Fig. 6: The data statistics of P2Med-MD. (a) The distribution of gender. (b) The distribution of age (in years). (c) The diversity in image modalities. The collected dataset encompassed approximately 70K radiology images, spanning two modalities of varying dimensions: 2D for X-ray and 3D for CT scans. Note: P2Med-MD: Medical Multimodal Dataset for Pediatric Pneumonia. CT: Computed Tomography. AP: AnteroPosterior view. Lat: Lateral view. Non-Con: Non-Contrast series. CE: Contrast-Enhanced series.

sizes between 325 and 5,000. For three-level inpatient medical records, we included all samples from disease categories containing 40 to 500 samples. Fig. 7b, 7c, 7g, 7k, 7l, and 7m illustrated the distribution of disease categories for six tasks in stage 3, which were more balanced compared to stage 2.

5) Medical Multimodal Benchmark for Pediatric Pneumonia (P2Med-MBench): Building upon P2Med-MD, we presented P2Med-MBench, a comprehensive evaluation benchmark for pediatric pneumonia. P2Med-MBench contained six distinct tasks, including radiology report generation (X-ray), radiology report generation (CT), outpatient medical record generation, first disease course record generation, attending physician’s first ward round record generation, and chief physician’s first ward round record generation. A detailed breakdown of each task, including task description, clinical scenario, modality, image dimension, model input, and model output [44], was shown in Table VI.

It was noteworthy that the P2Med-MD was collected over a continuous period. It was diverse and complex, potentially even containing some data with noise. To guarantee the data quality and representativeness for evaluation, two pediatric pulmonology specialists performed meticulous manual verification of the P2Med-MBench samples. Ultimately, we

obtained 121 samples for radiology report generation (X-ray), 121 samples for radiology report generation (CT), 100 samples for outpatient medical record generation, 100 samples for first disease course record generation, 100 samples for attending physician’s first ward round record generation, and 100 samples for chief physician’s first ward round record generation. These samples were dismissed in the whole training set. Detailed descriptions of the six evaluation tasks were provided in the following.

Radiology report generation (X-ray). This task primarily focused on the automatic generation of radiology reports for X-ray images, encompassing two key sections: findings and impression. The former provided a detailed description of crucial aspects observed in the 2D X-ray images, while the latter summarized the most relevant findings. Given that an outpatient or inpatient might have one or more X-ray images taken from various views and different times, we incorporated time, modality, and corresponding multi-view images in the input to facilitate correlation and comparison with prior radiological data of the same patient, thereby enabling the generation of more objective and comprehensive radiology reports. For a given set of X-ray images, we employed prompt sentences similar to the following as input: “Current

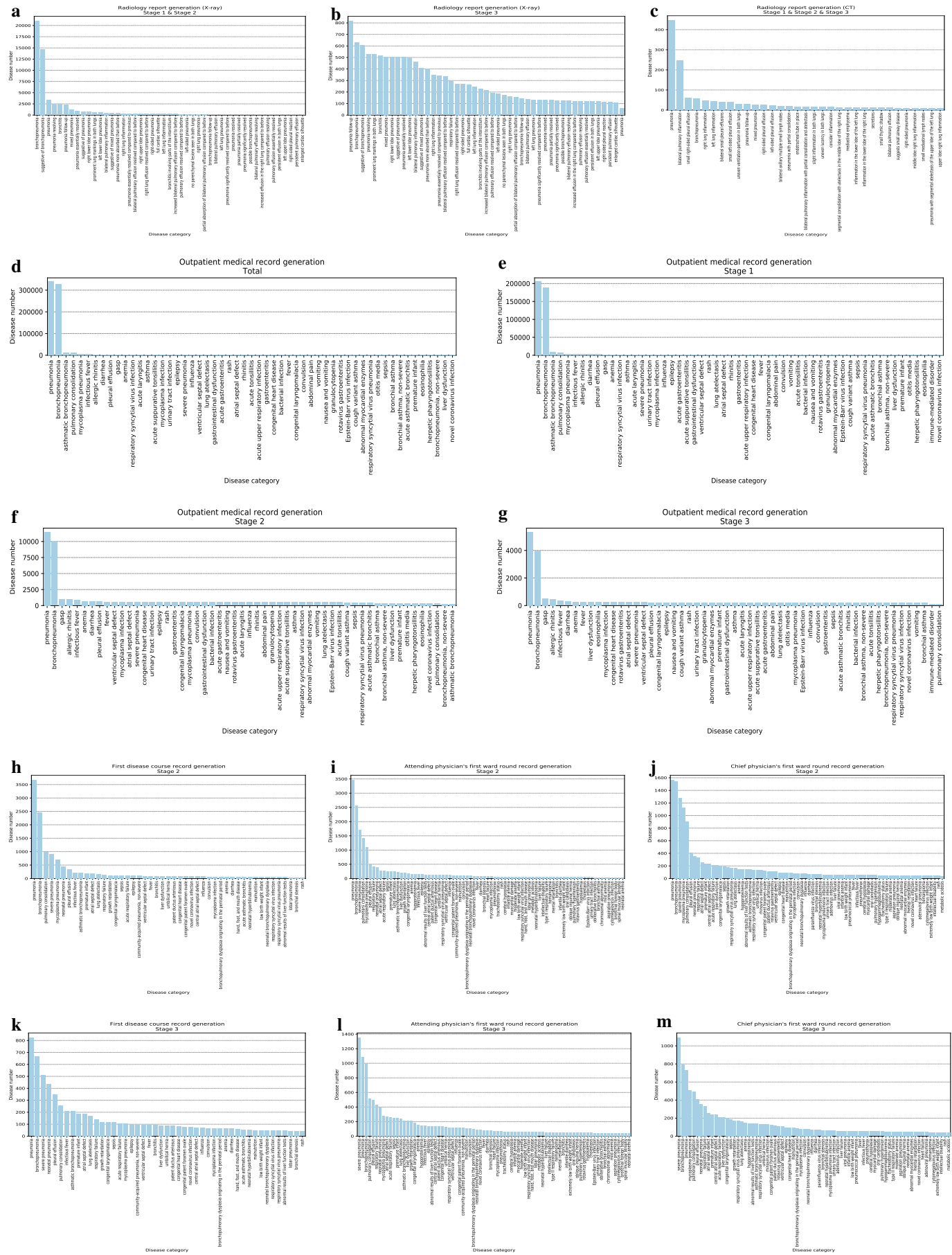


Fig. 7: The disease distribution of P2Med-MD across different stages and tasks. Stage 1 to stage 3 represented medical knowledge infusion pre-training, task type-based balanced instruction-tuning, and disease category-based balanced instruction-tuning, respectively. Note: P2Med-MD: Medical Multimodal Dataset for Pediatric Pneumonia. CT: Computed Tomography.

TABLE VI: Description of the P2Med-MBench.

Task number	Task description	Clinical scenario	Modality	Image modality	Image dimension	Model input	Model output
1	Radiology report generation (X-ray)	Outpatient / Inpatient	Image-text	X-ray	2D	Examination time + Examination modality + Image	Findings + Impression
2	Radiology report generation (CT)	Outpatient / Inpatient	Image-text	CT	3D	Examination time + Examination modality + Image	Findings + Impression
3	Outpatient medical record generation	Outpatient	Plain text	-	-	Chief complaint + History of present illness + Physical examination	Preliminary diagnosis + Treatment recommendation + Treatment plan
4	First disease course record generation	Inpatient	Plain text	-	-	History of present illness + Physical examination + Auxiliary examination + Clinical history features	Diagnostic basis + Admission diagnosis + Diagnostic and treatment plan
5	Attending physician's first ward round record generation	Inpatient	Plain text	-	-	Clinical history features + Additional clinical history and signs	Diagnostic basis + Current diagnosis + Diagnostic and treatment plan
6	Chief physician's first ward round record generation	Inpatient	Plain text	-	-	Clinical history features + Additional clinical history and signs	Diagnostic basis + Current diagnosis + Diagnostic and treatment plan

Note: P2Med-MBench: Medical Multimodal Benchmark for Pediatric Pneumonia. CT: Computed Tomography.

radiological data is as follows: $\backslash n$ [Examination time] December 31, 2022 $\backslash n$ [Examination modality] X-ray $\backslash n$ [Image] $\langle image \rangle \dots \langle image \rangle$ $\backslash n$ Based on the above information, combined with professional radiological knowledge, generate a report in the format: $\backslash n$ [Findings] {Your findings based on the images} $\backslash n$ [Impression] {Your impression based on the images} $\backslash n$ ". The number of $\langle image \rangle$ tokens corresponded to the number of views, with one for the anteroposterior view and two for the anteroposterior and lateral views. The impression, as the most critical component, was assessed using two metrics: accuracy and comprehensiveness, while the findings were evaluated solely on accuracy. To ensure the reliability of our evaluation, we have selected 100 sets of X-ray image-report pairs at unique time points and 10 sets at multiple times from the same patient, altogether comprising 121 samples and covering more than 47 distinct diseases.

Radiology report generation (CT). This task was similar to the radiology report generation (X-ray) task but was specifically designed for 3D CT images, thereby the examination modality was CT. The number of $\langle image \rangle$ tokens denoted the number of series, with one representing a non-contrast series, and two indicating both non-contrast and contrast-enhanced series. The final selection of 121 samples encompassed more than eight types of diseases.

Outpatient medical record generation. This task imitated the clinical process of a physician's outpatient visit, utilizing textual information such as the chief complaint, history of present illness, and physical examination to formulate a preliminary diagnosis, a treatment recommendation for the patient, and a treatment plan for the doctor. Here, we simulated this task as a prompt-based generative dialogue task. For example, we used the following as input: "Current outpatient pediatric information is as follows: $\backslash n$ [Chief complaint] The

pediatric patient presented with cough and fever for 4 days ... $\backslash n$ [History of present illness] Maximum temperature of 40°C ... $\backslash n$ [Physical examination] The pediatric patient is conscious and responsive ... $\backslash n$ Based on the above information, combined with professional medical knowledge, make a diagnosis in the format: $\backslash n$ [Preliminary diagnosis] {Your preliminary diagnosis} $\backslash n$ [Treatment recommendation] {Your treatment recommendation} $\backslash n$ [Treatment plan] {Your treatment plan} $\backslash n$ ". The output was then matched with the ground truth. The preliminary diagnosis, the most crucial element, was assessed on both accuracy and comprehensiveness, while the treatment recommendation and treatment plan were evaluated only on accuracy. We have selected 100 samples covering more than 55 disease types for preliminary diagnosis.

First disease course record generation. This task simulated the process by which a resident physician recorded the first disease course for a patient within 24 hours of hospitalization, synthesizing textual information such as history of present illness, physical examination, auxiliary examination, and clinical history features to predict the diagnostic basis, admission diagnosis, and diagnostic and treatment plan. The diagnostic basis explained the causes related to the admission diagnosis, reflecting the model's capacity for logical reasoning. We employed prompt sentences like "Current inpatient pediatric information is as follows: $\backslash n$ [History of present illness] The pediatric patient had a fever without obvious inducement five days ago (October 9, 2023) ... $\backslash n$ [Physical examination] The pediatric patient is conscious and responsive ... $\backslash n$ [Auxiliary examination] October 9, 2023: outpatient blood test ... $\backslash n$ [Clinical history features] Male, 13 years old ... $\backslash n$ Based on the above information, combined with professional medical knowledge, make a diagnosis in the format: $\backslash n$ [Diagnostic basis] {Your diagnostic basis} $\backslash n$ [Admission

diagnosis] {*Your admission diagnosis*} \n [*Diagnostic and treatment plan*] {*Your diagnostic and treatment plan*} \n” as input. We focused primarily on the admission diagnosis, evaluating it for both accuracy and comprehensiveness, while the diagnostic basis and diagnostic and treatment plan were assessed only for accuracy. Similarly, we have selected 100 samples that include more than 47 types of diseases for admission diagnosis.

Attending physician’s first ward round record generation. This task simulated how an attending physician performed the first ward round within 72 hours of a patient’s hospitalization, analyzing textual data such as clinical history features and additional clinical history and signs to predict the diagnostic basis, current diagnosis, and diagnostic and treatment plan. We utilized the following prompt as input: “*Current inpatient pediatric information is as follows:* \n [*Clinical history features*] *Male, 13 years old ...* \n [*Additional clinical history and signs*] *The pediatric patient continues to experience recurrent fever, peaking at 39.7°C ...* \n *Based on the above information, combined with professional medical knowledge, make a diagnosis in the format:* \n [*Diagnostic basis*] {*Your diagnostic basis*} \n [*Current diagnosis*] {*Your current diagnosis*} \n [*Diagnostic and treatment plan*] {*Your diagnostic and treatment plan*} \n”. Our primary focus was on the current diagnosis, thus we evaluated the prediction using accuracy and comprehensiveness, while the diagnostic basis and the diagnostic and treatment plan were assessed solely on accuracy. Similarly, we have selected 100 samples, covering over 79 types of diseases for current diagnosis.

Chief physician’s first ward round record generation. This task was similar to the attending physician’s first ward round record generation task; however, it specifically simulated the chief physician’s first ward round record within one week of a patient’s hospitalization. The selected 100 samples encompassed more than 74 types of diseases for current diagnosis.

B. Medical Multimodal Large Language Model for Pediatric Pneumonia (P2Med-MLLM)

As illustrated in Fig. 8, the architecture of the **Medical Multimodal Large Language Model for Pediatric Pneumonia (P2Med-MLLM)** primarily consisted of three modules: a pre-trained LLM (*e.g.*, Chinese-LLaMA-2 [31], [45]) serving as the foundational model, a pre-trained vision encoder (*e.g.*, CLIP [32]) responsible for encoding medical images into image embeddings, and an attention-based perceiver [7] that transformed these image embeddings into image tokens compatible with the LLM.

For P2Med-MLLM training, we considered a three-stage procedure, shown in Fig. 1a. During the first stage of medical knowledge fusion pre-training, only the perceiver module was trainable, facilitating the alignment of multimodal features. Subsequently, during the second and third stages of instruction-tuning, the LLM employed Low-Rank Adaptation (LoRA) [46] for efficient parameter tuning. All medical data were formatted as either a single-round conversation (plain text and image-text paired data) or multi-round conversations (interleaved image-text data) for model training.

Next, we would provide a detailed introduction to the P2Med-MLLM.

1) *Efficient Large Language Model Finetuning:* The LLM pre-trained on web datasets lacked the vertical domain knowledge required for pediatric pneumonia, leading to suboptimal performance for corresponding medical tasks. It was essential to update the LLM parameters using medical data. Due to constraints in computational resources, finetuning the full parameters of the LLM, which consisted of 7B parameters, was unfeasible. To address these challenges, we adopted LoRA for efficient parameter tuning.

LoRA introduced low-rank matrices, denoted as A and B , which had a significantly smaller number of parameters than the original model weights. The adaptation was formulated as:

$$W' = W + \Delta W \quad (1)$$

where W was the original weight matrix, and ΔW was the low-rank update defined as:

$$\Delta W = AB^T \quad (2)$$

where $A \in \mathbb{R}^{d \times r}$ and $B \in \mathbb{R}^{d \times r}$, with r being the rank which was much smaller than d , the dimension of W . T represented the transpose operation.

By training only the low-rank matrices A and B while keeping the original LLM parameters frozen, we achieved efficient optimization with significantly reduced computational overhead. The lightweight nature of these low-rank matrices ensured that there was almost no additional inference latency introduced during the inference stage. Ultimately, we efficiently incorporated critical medical knowledge into the LLM, enhancing its performance in this specialized field without the need for extensive computational resources.

2) *2D/3D Medical Image Perception:* Traditional approaches typically employed a linear projection [11], [24] or a Multi-Layer Perceptron (MLP) [12] as the cross-modal connector to convert medical image embeddings into visual tokens for being integrated into LLM. However, these conventional methods encountered significant challenges when processing 3D CT images, which typically consisted of more than 30 slices. The conversion of these images resulted in an excessively large number of visual tokens, far exceeding the LLM’s maximum token limit. For instance, a 2D image was encoded as 576 visual tokens, whereas a 3D image with 30 slices was encoded as $30 \times 576 = 17,280$ visual tokens, which far exceeded the typical LLM maximum length of 4,096 tokens.

To address this challenge, we utilized a lightweight Transformer decoder-only [47] structure based on the attention mechanism, named as the perceiver module [7], [48], to simultaneously process 2D/3D medical images embeddings into a fixed number of visual tokens. Specifically, the perceiver first incorporated learnable temporal and positional embeddings into the image embeddings, which were then flattened for injecting into the attention layer. The attention layer operates were as follows:

$$Q = W^Q h, K = W^K x, V = W^V x \quad (3)$$

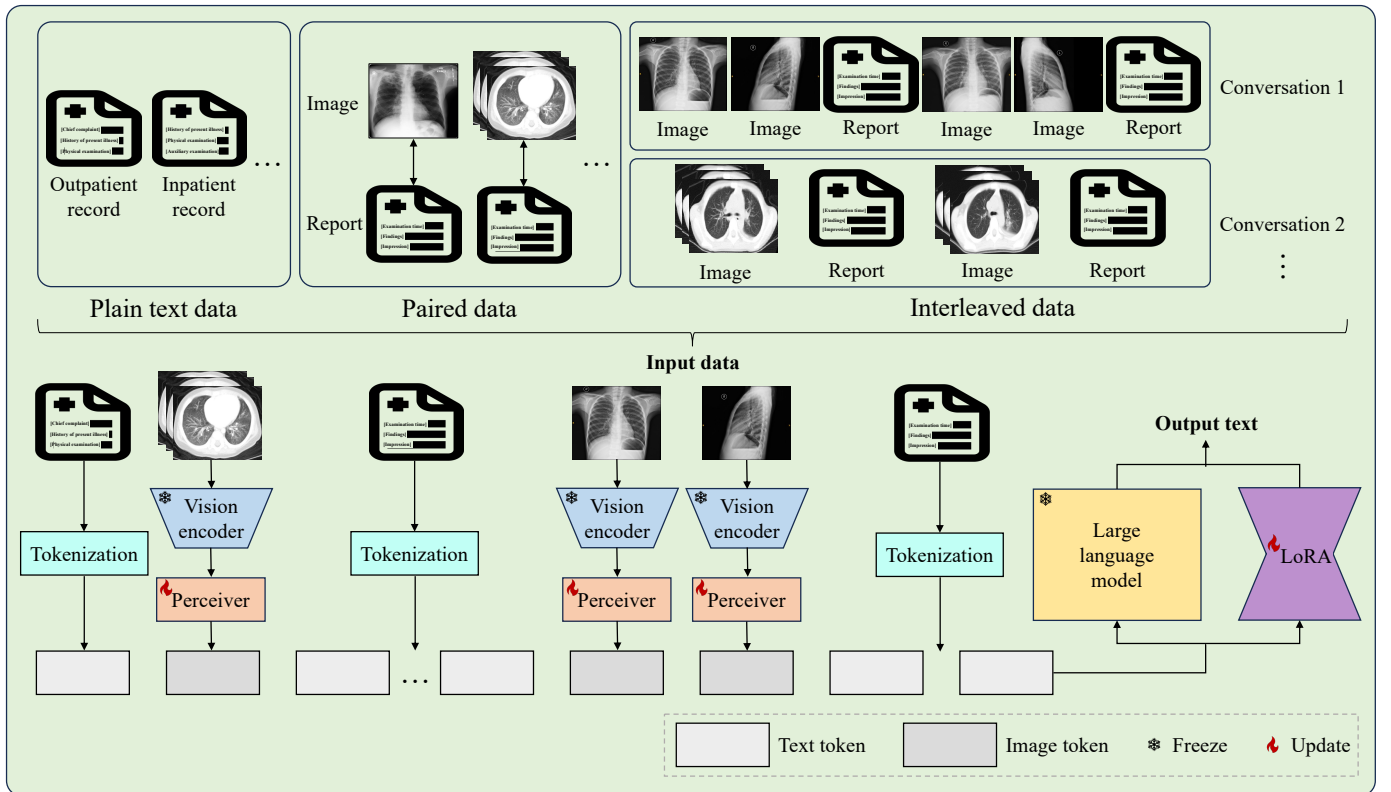


Fig. 8: The framework of our P2Med-MLLM. It can process plain text, medical image-report pairs, and multiple 2D or 3D images interleaved with medical reports. Note: P2Med-MLLM: Medical Multimodal Large Language Model for Pediatric Pneumonia.

where h represented the learnable latent array, while x corresponded to the flattened visual features. Q , K , and V denoted the query, key, and value vectors used in cross-attention interactions. W^Q , W^K , and W^V were learned weight matrices.

The attention mechanism then computed:

$$\text{Attention}(Q, K, V) = \text{softmax}\left(\frac{QK^T}{\sqrt{d_k}}\right)V \quad (4)$$

where d_k was the dimension of the key vector.

Ultimately, through this unified architecture, the perceiver module efficiently processed the perception of both 2D and 3D medical images, ensuring that the resulting visual tokens were compatible in length with the LLM. This approach optimized the integration of complex medical imaging data with the LLM, making it suitable for advanced medical tasks.

3) Multimodal Medical Data Formats: The medical data collected for training were categorized into plain text data and multimodal data. Each data instance input X_i and output X_o were reformatted into an instruction-following structure:

$$\text{Human: } X_p X_i^1 \langle \text{STOP} \rangle \text{ Assistant: } X_o^1 \langle \text{STOP} \rangle$$

where X_p referred predefined instructional prompts for different tasks. Please see Sec V-A.5 for the illustrations of different prompts. The model was designed to predict the assistant's responses and where to stop. Therefore, only **green tokens** were used to calculate the training loss.

For the plain text data, which primarily concerned record generation, X_i referred to patient-specific information, while X_o consisted of the resultant medical records. In the context of

multimodal medical image-report data, the input X_i referred to visual data such as X-ray or CT images, and X_o consisted of the findings and impressions, interpreting and summarizing the visual observations. Qualitative examples illustrating our data formats were shown in Fig. 3. For the original Chinese version, please refer to Fig. S2.

The analysis of the collected data revealed that a patient sometimes underwent multiple radiological examinations, resulting in correlated medical image-report pairs. For instance, sequential reports may contain comparisons such as “*Compared to the scan from October 29, 2022, both lungs show ...*”. Treating each medical image-report pair as an independent instruction instance can hinder the model's ability to recognize relationships across a patient's sequential image-report data. To mitigate this limitation, we converted multiple related image-report pairs of a patient into an interleaved data format:

$$\begin{aligned} \text{Human: } X_p X_i^1 \langle \text{STOP} \rangle \text{ Assistant: } X_o^1 \langle \text{STOP} \rangle, \\ \text{Human: } X_p X_i^2 \langle \text{STOP} \rangle \text{ Assistant: } X_o^2 \langle \text{STOP} \rangle \dots \end{aligned}$$

This approach enabled our model to consider all previously associated image-report data when generating new reports.

C. Training Details

1) Data Preprocessing: In the analysis of medical imaging and textual data for pediatric pneumonia, we initially identified all patient-related information. For the preprocessing of 2D chest X-ray images, each chest X-ray examination retained either an anteroposterior view or both anteroposterior and lateral views, and the x-axis and y-axis were resized to

336 pixels. For the preprocessing of 3D chest CT images, we selected lung reconstruction series with a slice thickness of 5.0 mm and normalized them based on a window level of -500 HU and a window width of 1,200 HU. Each chest CT examination retained either a non-contrast series or both non-contrast and contrast-enhanced series, and the x-axis and y-axis were resized to 336 pixels. When the z-axis dimensions of non-contrast and contrast-enhanced series differed, the shorter one was padded with zeros to match. For the preprocessing of textual data including medical reports, outpatient, and inpatient records, we removed records with any missing element in the model’s ground truth output. Additionally, we excluded records containing over 4,000 tokens, as their excessive lengths hindered the effective learning of the LLM. Specifically, for deduplication of outpatient records, we utilized 5-grams with a Jaccard similarity threshold of 0.85, 16 rows, and 256 bands. Meanwhile, we filtered out outpatient records with n-grams less than 5.

2) *Implementation*: We utilized a 24-layer, 2D ViT-L/14 with 1,024 embedding dimensions as the vision encoder, initialized with CLIP weights. The perceiver was a 6-layer transformer decoder with a learnable latent array of $32 \times 4,096$ dimensions. For the LLM, we employed the 32-layer, 7B Chinese-LLaMA-2. Our final model comprised 8B parameters. During the three training stages, we froze the vision encoder and LLM, updating only the perceiver and LoRA parameters. All models were implemented in PyTorch and trained on 8 NVIDIA A6000 GPUs with 48 GB memory each. To prevent gradient errors during backpropagation, each batch during training samples was either image-text pairs or plain text data. For optimization, we used the Adam optimizer with a cosine decay scheduler and a warmup ratio of 0.03. Detailed hyperparameters were provided in Table VII.

TABLE VII: P2Med-MLLM hyperparameters. Stage 1 to stage 3 represented medical knowledge infusion pre-training, task type-based balanced instruction-tuning, and disease category-based balanced instruction-tuning, respectively.

Stage	Epoch	Training time	Max tokens	Learning rate	Batch size per device	Gradient accumulation
1	1	15 hours	2,048	2×10^{-6}	2	1
2	4	19 hours	4,096	2×10^{-6}	1	16
3	4	8 hours	4,096	2×10^{-7}	1	16

Note: P2Med-MLLM: Medical Multimodal Large Language Model for Pediatric Pneumonia.

REFERENCES

- [1] M. Roser, H. Ritchie, and B. Dadonaite, “Child and infant mortality,” *Our world in data*, 2021. [Online]. Available: <https://ourworldindata.org/child-mortality>
- [2] C. Ebeledike and T. Ahmad, “Pediatric pneumonia,” *StatPearls*, 2022.
- [3] G. Yu *et al.*, “Identification of pediatric respiratory diseases using a fine-grained diagnosis system,” *Journal of Biomedical Informatics*, vol. 117, p. 103754, 2021.
- [4] G. Yu *et al.*, “The role of artificial intelligence in identifying asthma in pediatric inpatient setting,” *Annals of translational medicine*, vol. 8, no. 21, 2020.
- [5] W. Liang *et al.*, “Early triage of critically ill covid-19 patients using deep learning,” *Nature communications*, vol. 11, no. 1, p. 3543, 2020.
- [6] H.-Y. Zhou *et al.*, “A transformer-based representation-learning model with unified processing of multimodal input for clinical diagnostics,” *Nature Biomedical Engineering*, pp. 1–13, 2023.
- [7] J.-B. Alayrac *et al.*, “Flamingo: a visual language model for few-shot learning,” *Advances in neural information processing systems*, vol. 35, pp. 23 716–23 736, 2022.
- [8] A. Awadalla *et al.*, “Openflamingo: An open-source framework for training large autoregressive vision-language models,” *arXiv preprint arXiv:2308.01390*, 2023.
- [9] Z. Yang *et al.*, “The dawn of llms: Preliminary explorations with gpt-4v (ision),” *arXiv preprint arXiv:2309.17421*, vol. 9, no. 1, p. 1, 2023.
- [10] S. Wu, H. Fei, L. Qu, W. Ji, and T.-S. Chua, “Next-gpt: Any-to-any multimodal llm,” *arXiv preprint arXiv:2309.05519*, 2023.
- [11] H. Liu, C. Li, Q. Wu, and Y. J. Lee, “Visual instruction tuning,” *Advances in neural information processing systems*, vol. 36, 2024.
- [12] H. Liu, C. Li, Y. Li, and Y. J. Lee, “Improved baselines with visual instruction tuning,” in *Proceedings of the IEEE/CVF Conference on Computer Vision and Pattern Recognition*, 2024, pp. 26 296–26 306.
- [13] C. Wu *et al.*, “Can gpt-4v (ision) serve medical applications? case studies on gpt-4v for multimodal medical diagnosis,” *arXiv preprint arXiv:2310.09909*, 2023.
- [14] M. Moor *et al.*, “Med-flamingo: a multimodal medical few-shot learner,” in *Machine Learning for Health (ML4H)*. PMLR, 2023, pp. 353–367.
- [15] F. Liu *et al.*, “A medical multimodal large language model for future pandemics,” *NPJ Digital Medicine*, vol. 6, no. 1, p. 226, 2023.
- [16] C. Wu, X. Zhang, Y. Zhang, Y. Wang, and W. Xie, “Towards generalist foundation model for radiology,” *arXiv preprint arXiv:2308.02463*, 2023.
- [17] J. Liu, Z. Wang, Q. Ye, D. Chong, P. Zhou, and Y. Hua, “Qilin-med-vl: Towards chinese large vision-language model for general healthcare,” *arXiv preprint arXiv:2310.17956*, 2023.
- [18] J. Zhou, X. Chen, and X. Gao, “Path to medical agi: Unify domain-specific medical llms with the lowest cost,” *medRxiv*, pp. 2023–06, 2023.
- [19] J. Zhou *et al.*, “Skingpt-4: an interactive dermatology diagnostic system with visual large language model,” *arXiv preprint arXiv:2304.10691*, 2023.
- [20] W. Gao *et al.*, “Ophglm: Training an ophthalmology large language-and-vision assistant based on instructions and dialogue,” *arXiv preprint arXiv:2306.12174*, 2023.
- [21] S. Xu *et al.*, “Elixir: Towards a general purpose x-ray artificial intelligence system through alignment of large language models and radiology vision encoders,” *arXiv preprint arXiv:2308.01317*, 2023.
- [22] S. Lee, W. J. Kim, J. Chang, and J. C. Ye, “Llm-cxr: Instruction-finetuned llm for cxr image understanding and generation,” in *The Twelfth International Conference on Learning Representations*, 2024.
- [23] T. Tu *et al.*, “Towards generalist biomedical ai,” *NEJM AI*, vol. 1, no. 3, p. AIoa2300138, 2024.
- [24] C. Li *et al.*, “Llava-med: Training a large language-and-vision assistant for biomedicine in one day,” *Advances in Neural Information Processing Systems*, vol. 36, 2024.
- [25] T. Tu *et al.*, “Towards conversational diagnostic ai,” *arXiv preprint arXiv:2401.05654*, 2024.
- [26] M. Y. Lu *et al.*, “A multimodal generative ai copilot for human pathology,” *Nature*, pp. 1–3, 2024.
- [27] J. Li *et al.*, “Integrated image-based deep learning and language models for primary diabetes care,” *Nature Medicine*, pp. 1–11, 2024.
- [28] Z. Zhao *et al.*, “Chatcad+: Towards a universal and reliable interactive cad using llms,” *IEEE Transactions on Medical Imaging*, 2024.
- [29] S. Bannur *et al.*, “Maira-2: Grounded radiology report generation,” *arXiv preprint arXiv:2406.04449*, 2024.
- [30] J. Ying *et al.*, “Comparative analysis of the three-level rounds system and responsible physician rounds system,” *Chinese Health Quality Management*, vol. 28, no. 2, pp. 03–05, 2021.
- [31] Y. Cui, Z. Yang, and X. Yao, “Efficient and effective text encoding for chinese llama and alpaca,” *arXiv preprint arXiv:2304.08177*, 2023.
- [32] A. Radford *et al.*, “Learning transferable visual models from natural language supervision,” in *International conference on machine learning*. PMLR, 2021, pp. 8748–8763.
- [33] A. Yang *et al.*, “Baichuan 2: Open large-scale language models,” *arXiv preprint arXiv:2309.10305*, 2023.
- [34] D. Hernandez *et al.*, “Scaling laws and interpretability of learning from repeated data,” *arXiv preprint arXiv:2205.10487*, 2022.
- [35] L. B. Allal *et al.*, “Santacoder: don’t reach for the stars!” *arXiv preprint arXiv:2301.03988*, 2023.
- [36] K. Lee *et al.*, “Deduplicating training data makes language models better,” *arXiv preprint arXiv:2107.06499*, 2021.

- [37] G. Penedo *et al.*, “The refinedweb dataset for falcon llm: outperforming curated corpora with web data, and web data only,” *arXiv preprint arXiv:2306.01116*, 2023.
- [38] Y. Li *et al.*, “Competition-level code generation with alphacode,” *Science*, vol. 378, no. 6624, pp. 1092–1097, 2022.
- [39] E. Nijkamp *et al.*, “Codegen: An open large language model for code with multi-turn program synthesis,” *arXiv preprint arXiv:2203.13474*, 2022.
- [40] D. Fried *et al.*, “InCoder: A generative model for code infilling and synthesis,” *arXiv preprint arXiv:2204.05999*, 2022.
- [41] D. Kocetkov *et al.*, “The stack: 3 tb of permissively licensed source code,” *arXiv preprint arXiv:2211.15533*, 2022.
- [42] L. Tunstall, L. Von Werra, and T. Wolf, *Natural language processing with transformers*. O’Reilly Media, Inc., 2022.
- [43] A. Z. Broder, “Identifying and filtering near-duplicate documents,” in *Annual symposium on combinatorial pattern matching*. Springer, 2000, pp. 1–10.
- [44] W. Wang, K. Sun, and L. Chang, *Pediatrics (9th edition)*. People’s Medical Publishing House, 2019.
- [45] H. Touvron *et al.*, “Llama 2: Open foundation and fine-tuned chat models,” *arXiv preprint arXiv:2307.09288*, 2023.
- [46] E. J. Hu *et al.*, “Lora: Low-rank adaptation of large language models,” in *International Conference on Learning Representations*, 2021.
- [47] A. Vaswani *et al.*, “Attention is all you need,” *Advances in neural information processing systems*, vol. 30, 2017.
- [48] J. Li, D. Li, S. Savarese, and S. Hoi, “Blip-2: Bootstrapping language-image pre-training with frozen image encoders and large language models,” in *International conference on machine learning*. PMLR, 2023, pp. 19 730–19 742.

SUPPLEMENTARY MATERIALS

指令: 你是一个专业的呼吸科放射学医生, 我希望你对于医生撰写的影像放射学表现, 与AI自动生成的影像放射学表现进行比较与评价, 并对AI生成的影像放射学表现的准确性进行打分。

在评价AI自动生成的放射学表现时, 需要考虑AI系统的描述是否符合患者影像的实际病情与症状。

以医生撰写的影像放射学表现为Ground Truth作为5分, 你需要对AI自动生成的放射学表现的准确性做出分析并给出分数, 分数范围为1-5分。

1分: AI报告中的信息完全错误, 与临床实际严重不符

2分: AI报告中有多处明显错误, 需要重新更正

3分: AI报告中大约一半的信息正确, 但包含几个错误, 需要进行核实

4分: AI报告大部分信息准确, 但可能包含少量不影响整体理解的错误或遗漏

5分: AI报告提供的医学信息与医生临床判断完全一致

输入:

[医生放射学表现]

胸廓对称, 气管居中, 两肺纹理增多、增粗, 双下肺见斑片状渗出影, 纵隔居中, 轮廓无殊, 心影不大, 两膈面光整、压低, 肋膈角锐利。

[AI生成放射学表现]

胸廓对称, 气管居中, 两肺纹理增多、增粗, 右下肺见斑片状渗出影, 肺门影不大, 肺门角清晰, 纵隔居中, 轮廓无殊, 心影不大, 两膈面光整, 肋膈角锐利。

输出:

[准确性分析] AI生成的描述中包含了“胸廓对称”、“气管居中”、“两肺纹理增多、增粗”、“右下肺见斑片状渗出影”等关键描述, 遗漏了“左下肺见斑片状渗出影”这一关键描述, 整体描述较为准确。

[准确性打分] 4

输入:

[医生放射学表现]

双肺透亮度正常, 右肺中叶及两肺下叶可见渗出影。气管及支气管通畅。纵隔内未见明显肿大淋巴结影。未见明显气胸、胸腔积液征象。

[AI生成放射学表现]

双肺透亮度不均, 两肺见多发斑片状渗出影。气管及支气管通畅。纵隔内未见明显肿大淋巴结影。未见明显气胸、胸腔积液征象。

输出:

Fig. S1: Illustration of the evaluation process (Chinese version). We evaluated model-generated answers using 13B Chinese-LLaMA-2.

Task	Input prompt	P2Med-MLLM prediction	Ground truth
Radiology report generation (X-ray)	<p>目前有放射学信息如下： 【检查时间】 2022.10.29 【检查状态】 X-ray 【图像】 <image> 基于以上信息，结合专业放射学知识生成报告，请按以下格式回复： 【放射学表现】 {你的放射学表现} 【放射学诊断】 {你的放射学诊断}</p>	<p>【放射学表现】 两肺纹理增多、增粗，右下肺内带见斑片状阴影，纵膈居中。 【放射学诊断】 肺炎，两肺内见斑片状阴影，纵膈居中。 【放射学诊断】 提示支气管炎。</p>	<p>【放射学表现】 两肺纹理增多、增粗，右下肺内带见斑片状阴影，纵膈居中。 【放射学诊断】 肺炎，两肺内见斑片状阴影，纵膈居中。纵膈居中，轮廓无殊，心影不大，两肺野清晰，肋膈角锐利。 【放射学诊断】 提示支气管炎。</p>
	<p>目前有放射学信息如下： 【检查时间】 2022.11.11 【检查状态】 X-ray 【图像】 <image> 基于以上信息，结合专业放射学知识生成报告，请按以下格式回复： 【放射学表现】 {你的放射学表现} 【放射学诊断】 {你的放射学诊断}</p>	<p>【放射学表现】 两肺纹理增多、增粗，右下肺内带见斑片状阴影较2022.10.29。 【放射学诊断】 肺炎，两肺内见斑片状阴影，纵膈居中。 【放射学诊断】 提示支气管炎。</p>	<p>【放射学表现】 两肺纹理增多、增粗，右下肺内带见斑片状阴影较2022.10.29。 【放射学诊断】 肺炎，两肺内见斑片状阴影，纵膈居中。纵膈居中，轮廓无殊，心影不大，两肺野清晰，肋膈角锐利。 【放射学诊断】 提示支气管炎。</p>
Radiology report generation (CT)	<p>目前有放射学信息如下： 【检查时间】 2021.3.25 【检查状态】 CT 【图像】 <image> 基于以上信息，结合专业放射学知识生成报告，请按以下格式回复： 【放射学表现】 {你的放射学表现} 【放射学诊断】 {你的放射学诊断}</p>	<p>【放射学表现】 双肺透亮度不均，两肺见斑片状阴影，气管及支气管增粗，纵膈未见明显肿大淋巴结，未见明显气胸、胸腔积液征。 【放射学诊断】 肺炎。</p>	<p>【放射学表现】 双肺透亮度不均，可见多发斑片状阴影，气管及支气管增粗，纵膈未见明显肿大淋巴结，未见明显气胸、胸腔积液征。 【放射学诊断】 肺炎。</p>
Outpatient medical record generation	<p>目前有门诊患儿信息如下： 【主诉】 肺炎反复。 【现病史】 患儿仍有发热，伴咳，有空呼吸音，精神稍软，夜眠可。 【体格检查】 患儿神志清，反应可，唇红，气平，双肺呼吸音粗，可及痰鸣音。心音有力，律齐，全腹软，未及压痛，肝脾不大，肠鸣音不亢进，NS (-)。 基于以上信息，结合专业医学知识做出诊断，请按如下格式回复： 【初步诊断】 {你的初步诊断} 【处理意见】 {你的处理意见} 【治疗计划】 {你的治疗计划}</p>	<p>【初步诊断】 肺炎，急性肺炎。 【处理意见】 1、健康宣教，注意清淡饮食，多喝水，勤拍背，避免交叉感染。 【治疗计划】 2、继续口服头孢、高热不退、精神反应差等及时就诊。</p>	<p>【初步诊断】 肺炎，急性肺炎。 【处理意见】 1、多喝水，清淡饮食。2、接种、戒烟、气促、神疲等。 【治疗计划】 1、检查：CT-胸部CT扫描。</p>
First disease course record generation	<p>目前有住院患儿信息如下： 【现病史】 患儿（2023.10.1）9天前无明显诱因出现阵发性咳嗽... 【体格检查】 患儿神清，精神反应可，呼吸平，皮肤弹性可，未见皮疹，口唇无绀，未见三凹征。心音有力，律齐，未闻及病理性杂音。双肺呼吸运动对称，两肺触觉语颤正常... 【辅助检查】 2023.10.1 胸部X-ray: 支气管炎。2023.10.1 血常规: CRP < 8 mg/L, WBC 10.8*10⁹/L。2023.10.3 胃肠彩超: 肠系膜淋巴结肿大。目前超声可见范围内腹腔内未见明显局限性包块... 【病史特点】 1、男，6月13天... 基于以上信息，结合专业医学知识做出诊断，请按如下格式回复： 【诊断依据】 {你的诊断依据} 【入院诊断】 {你的入院诊断} 【治疗计划】 {你的治疗计划}</p>	<p>【诊断依据】 患儿阵发性咳嗽，起病急，病程13天，因“咳嗽、气促”入院。体格检查：神清，精神反应可，口唇无绀，未见三凹征，心音有力，律齐，未闻及病理性杂音。双肺呼吸运动对称，两肺触觉语颤正常。辅助检查：胸部X-ray提示支气管炎。肝脾不大，肠鸣音正常。神经查体阴性(-)。胸部X-ray提示支气管炎。 【入院诊断】 喘息性支气管炎。 【治疗计划】 1、对症支持治疗。2、雾化吸入治疗。3、三大常规、生化、血常规、痰培养、痰病原学、呼吸道病毒学等。4、予以吸氧及雾化吸入治疗。5、根据病情变化调整治疗方案。</p>	<p>【诊断依据】 喘息性支气管炎。患儿6月龄男婴，因“阵发性咳嗽、气促”入院。体格检查：神清，精神反应可，口唇无绀，未见三凹征，心音有力，律齐，未闻及病理性杂音。双肺呼吸运动对称，两肺触觉语颤正常。辅助检查：胸部X-ray提示支气管炎。肝脾不大，肠鸣音正常。神经查体阴性(-)。胸部X-ray提示支气管炎。 【入院诊断】 喘息性支气管炎。 【治疗计划】 1、对症支持治疗。2、雾化吸入治疗。3、三大常规、生化、血常规、痰培养、痰病原学、呼吸道病毒学等。4、予以吸氧及雾化吸入治疗。5、根据病情变化调整治疗方案。</p>
Attending physician's first ward round record generation	<p>目前有住院患儿信息如下： 【病史特点】 1、因“咳嗽、流涕3天”入院。2、现病史：患儿为孕38+5周... 3、体格检查：足月儿貌，反应可... 4、辅助检查：2023.10.13 血常规急诊：C反应蛋白<8 mg/L；血红蛋白130 g/L... 【补充病史体征】 患儿鼻导管吸氧下血氧稳定，仍咳嗽痰喘，无气促，无发热，抽搐，奶量完成，无恶心、呕吐，大小便正常。体格检查：轻度充血。 基于以上信息，结合专业医学知识做出诊断，请按如下格式回复： 【诊断依据】 {你的诊断依据} 【当前诊断】 {你的当前诊断} 【治疗计划】 {你的治疗计划}</p>	<p>【诊断依据】 新生儿肺炎。患儿为孕38+5周，出生体重3150克。入院第3天接触“支原体肺炎”姐姐后，出现咳嗽、痰喘较前加重。有痰，不伴有发热。体格检查：双肺呼吸音粗，可闻及痰鸣音及少许湿啰音。结合胸部X-ray结果，故诊断。 【治疗计划】 1、予心电、血氧监护。2、雾化吸入治疗。3、予以吸氧及雾化吸入治疗。4、根据病情变化调整治疗方案。</p>	<p>【诊断依据】 新生儿肺炎。患儿6月龄男婴，因“阵发性咳嗽、气促”入院。体格检查：神清，精神反应可，口唇无绀，未见三凹征，心音有力，律齐，未闻及病理性杂音。双肺呼吸运动对称，两肺触觉语颤正常。辅助检查：胸部X-ray提示支气管炎。肝脾不大，肠鸣音正常。神经查体阴性(-)。胸部X-ray提示支气管炎。 【当前诊断】 新生儿肺炎。 【治疗计划】 1、心电、血氧监护等。2、雾化吸入治疗。3、予以吸氧及雾化吸入治疗。4、根据病情变化调整治疗方案。</p>
Chief physician's first ward round record generation	<p>目前有住院患儿信息如下： 【病史特点】 1、患儿，女，1月25天... 2、现病史：患儿5天前无明显诱因出现阵发性咳嗽... 3、体格检查：患儿神志清，精神反应可... 4、辅助检查：2021.12.22 血气（新生儿）：C-LAC乳酸浓度2.7 mmol/L... 【补充病史体征】 患儿鼻导管吸氧下血氧稳定，仍咳嗽痰喘，无气促，无发热，抽搐，奶量完成，无恶心、呕吐，大小便正常。体格检查：轻度充血。4.14ml/kg/h。 基于以上信息，结合专业医学知识做出诊断，请按如下格式回复： 【诊断依据】 {你的诊断依据} 【当前诊断】 {你的当前诊断} 【治疗计划】 {你的治疗计划}</p>	<p>【诊断依据】 支气管炎肺炎。患儿，女，1月25天，因“阵发性咳嗽、痰喘”入院。体格检查：神清，精神反应可，口唇无绀，未见三凹征，心音有力，律齐，未闻及病理性杂音。双肺呼吸运动对称，两肺触觉语颤正常。辅助检查：胸部X-ray提示支气管炎。肝脾不大，肠鸣音正常。神经查体阴性(-)。胸部X-ray提示支气管炎。 【当前诊断】 喘息性支气管炎。 【治疗计划】 1、对症支持治疗。2、雾化吸入治疗。3、三大常规、生化、血常规、痰培养、痰病原学等。4、予以吸氧及雾化吸入治疗。5、根据病情变化调整治疗方案。</p>	<p>【诊断依据】 支气管炎肺炎。患儿6月龄男婴，因“阵发性咳嗽、气促”入院。体格检查：神清，精神反应可，口唇无绀，未见三凹征，心音有力，律齐，未闻及病理性杂音。双肺呼吸运动对称，两肺触觉语颤正常。辅助检查：胸部X-ray提示支气管炎。肝脾不大，肠鸣音正常。神经查体阴性(-)。胸部X-ray提示支气管炎。 【当前诊断】 喘息性支气管炎。 【治疗计划】 1、对症支持治疗。2、雾化吸入治疗。3、三大常规、生化、血常规、痰培养、痰病原学等。4、予以吸氧及雾化吸入治疗。5、根据病情变化调整治疗方案。</p>

Fig. S2: Qualitative examples of six different evaluation tasks (Chinese version). We presented input prompts along with answers generated by P2Med-MLLM and the target ground truth. The green color in the figure highlighted correct predictions, the red color indicated errors, and the blue color denoted neglected parts. Note: P2Med-MLLM: Medical Multimodal Large Language Model for Pediatric Pneumonia. CT: Computed Tomography.